Energy, Waste, and the Environment
A Geochemical Perspective

Editors: **Reto Gieré & Peter Stille** **Publisher:** **Geological Society, London**

VITRIFICATION OF DOMESTIC WASTES: EFFICIENT ENERGY UTILISATION FOR A SUSTAINABLE FUTURE?

D. PERRET[1,*], P. STILLE[2], J.-L. CROVISIER[2], G. SHIELDS[2,3], U. MÄDER[4], K. SCHENK[5], M. CHARDONNENS[5]

***** Corresponding author

1 Ecole Polytechnique Fédérale de Lausanne; Laboratoire de Pédologie; ENAC-ISTE-LPE; CH-1015 Lausanne, Switzerland; didier.perret@epfl.ch

2 ULP Ecole et Observatoire des Sciences de la Terre CNRS; Centre de Géochimie de la Surface UMR 7517; rue Blessig 1; F-67084 Strasbourg Cedex, France

3 James Cook University; School of Earth Sciences; Townsville; Queensland 4811, Australia AUS

4 Universität Bern; Mineralogisch-Petrographisches Institut; Balzerstrasse 1; CH-3012 Bern, Switzerland

5 Office Fédéral de l'Environnement, des Forêts et du Paysage; Division Déchets; CH-3003 Bern, Switzerland

Running title: Vitrification of domestic wastes

ABSTRACT

Advanced high-temperature technologies for the thermal treatment of municipal solid wastes or residues of conventional incineration produce vitrified materials which may have superior physical and chemical characteristics with respect to conventional residues (bottom ash, fly ash, filter cake). These materials, which may embed non-negligible concentrations of toxic metals, exhibit favourable thermodynamic durabilities and very low releases when subjected to corrosion. Within the frame of the increasing threat on our primary ressources, these materials could be envisioned as plausible secondary raw materials for future civil engineering applications, although their production is energy demanding. This Chapter presents the physical, chemical and microscopic characteristics of a large set of different vitrified materials originating from various high-temperature technologies; their behaviour under highly aggressive conditions of corrosion and their thermodynamic stability is also presented. It is concluded that these high-temperature materials are indeed highly favourable with respect to the environment.

1. VITRIFICATION: AN ALTERNATIVE ROUTE TO SECONDARY RAW MATERIALS

During the last two decades, environmentally sound waste management and treatment policies have come out to provide our societies with safer ways of disposing off our municipal solid wastes and residues. As an example, Switzerland has totally diverted its waste-landfilling policy of the 70's and 80's toward a global waste-incinerating policy, which has resulted in 2000 in the obligation to incinerate the entirety of non-recyclable municipal solid wastes (MSW; BUWAL, 1996), the incineration capacity of the country (*ca.* 3×10^6 t MSW/yr, resulting in *ca.* 750×10^3 t/yr bottom ashes, BA, *ca.* 46.5×10^3 t/yr fly ashes, FA, and *ca.* 11.625×10^3 t/yr filter cake, FC) being technically fulfilled for the next 25-30 years.

Emerging sustainable strategies for the long-term minimisation of the production of municipal solid wastes and residues of incineration are of actual concern, in particular in European countries and Japan, where MSW incineration was pioneeringly introduced because of limited landfill space. These strategies are mostly based on the separation of wastes at their place of production or at least prior to incineration, into fractions which can be easily recovered and recycled or converted into reuseable materials (e.g. ferrous and non-ferrous metals, glasses, recyclable plastics, paper and cardboard, compostable wastes), respectively fractions which must be treated separately because of their high toxicity (e.g. batteries, industrial toxic wastes, heavy metal rich sewage sludges, electronic and computer scraps). The main aims of these strategies are to reduce drastically the volumes of incinerable wastes and to feed conventional incineration plants with mostly, if not exclusively, non-recyclable and non-hazardous wastes, in order to produce the lowest possible masses of bottom ashes (BA), fly ashes (FA) and filter cakes (FC) that could eventually be landfilled without further treatment.

However, these strategies rely more on political, economical, behavioural and societal considerations than on technical limitations. As a consequence, the secondary residues (BA, FA, FC) of conventional MSW incinerators usually still contain high concentrations of toxic metals and cannot be reused as secondary raw materials or landfilled without pretreatments (e.g. inertisation into cement matrices) because of their highly reactive nature, in particular for the case of fly ashes (ABB-EAWAG-EMPA-KEZO, 1990; BUWAL, 1998; EKESA, 1992); the latter, which represent only 5-10% of the total mass of incineration residues, are a real threat to waste management policies. Indeed, efforts toward the reduction of non-desirable by-products in the life-cycle of goods must be continued and reinforced, but alternative routes to efficient waste treatment must also be explored.

A promising alternative for the optimisation of the complete cycle of resources-to-goods-to-residues is possibly available by means of several emerging advanced thermal treatment technologies. Operated at higher-than-conventional combustion temperatures (i.e. between 900°C and 1400°C) and thus being highly energy demanding, these technologies are claimed by their manufacturers to produce inert high-temperature materials (HT materials) with environmentally favourable characteristics (Thomé-Kozmiensky, 1994; Barin, 1991, 1992; Gutmann, 1996; Künstler *et al*., 1994; Schumacher and Gugat, 1994; Kanczarek *et al*., 1996; Patze, 1996; Stahlberg, 1996). While large endeavours have been invested in the last decade to design MSW incinerators with enhanced waste-to-energy ratios (actually up to 30% of the total energy yield, still continuing to improve), most conventional technologies still suffer on the side of the long-term quality of the residues they produce. Thus, it may be relevant from the point of view of the energy-to-waste-to-environment path to consider HT technologies as plausible options for a better management of the increasingly threatened ressources, as depicted on the schematic course of entropy of Figure 1.

FIGURE 1

An extra energy input into vitrification technologies, as compared to conventional incinerators which produce residual energy in the form of heat or electricity, may be considered as detrimental to the net energy balance of the complete ressources-to-wastes path. However, this additional energy requirement can also be considered as the additional price to pay for the long-term preservation of natural ressources, in particular in countries strongly relying on the importation of raw materials for the production of their domestic goods.

It is not the aim of this chapter to compare the extent of the environmental impact of non-reuseable incineration residues (BA, FA, FC), and the extra energy required by vitrification technologies to produce inert materials (Figure 1). Rather, this chapter is intended to bring supplementary information in the debate on the future policies on waste management and treatment, and on resources management. To be considered as sustainably relevant, HT materials should fulfil the following requirements:

1. The ratio [extra energy needed to produce HT materials]:[long-term environmental profit] should be as high as possible, at least higher than the equivalent ratio for the residues of conventional MSW incinerators. Discussion on this ratio is out of scope of the present chapter.

2. The intrinsic physico-chemical characteristics of HT materials, together with their leachability and long-term durability, should be as favourable as possible, at least globally more favourable than the characteristics of the equivalent residues of conventional MSW incinerators.

3. In case of re-use of HT materials as secondary raw materials, for instance in civil engineering applications, their mechanical characteristics should be comparable to the ones of the equivalent primary raw materials extracted from natural ressources.

The present chapter deals exclusively with the scientific issues of point 2 mentioned above. It is based on the results of a large study under the authority of the Swiss Agency for Environment, Forests and Landscape (SAEFL/BUWAL; Perret *et al.*, 2000, 2002, 2003). The in-depth survey was performed on 23 HT materials originating from 16 different advanced thermal treatment technologies developed by 10 different companies in Switzerland, Germany, France and Italy, and operated under realistic conditions (*e.g.* from wastes representative of average MSW). On the basis of the results, two scenarii are tested to assess the long-term behaviour of HT materials:

1. Landfill disposal of HT materials: This scenario is the most conservative, as it considers that HT materials are stable enough to be considered as inert materials which can be disposed off into specific landfills, hereafter referred to as "glassfills", requiring no special attention (*e.g.* technical barriers or precautionary monitoring of exfiltered waters).

2. Re-use of HT materials for civil engineering applications: This scenario, though more provocative than the previous one, complies with the principles of a sustainable management of natural ressources (Finet, 1994; Bottero *et al.*, 1997; Kraus and Meunier, 1997; O'Connor *et al.*, 1994; Yan and Neretnieks, 1995; Depmeier *et al.*, 1997; Zevenbergen *et al.*, 1994a, 1994b; Guyonnet *et al.*, 1998; Méhu, 1998). In this scenario, HT materials (instead of excavated natural materials) are re-used as foundation layers for road construction, hereafter referred to as "glassroad".

Indeed, the estimation of the release fluxes of metals from a hypothetical glassfill and a hypothetical glassroad will be based on experimental results and theoretical but realistic considerations.

2. THE GLOBAL PICTURE OF HT MATERIALS

This section is primarily intended to show that the relevant combination of the intrinsic physico-chemical and microscopie characteristics of HT materials, their behaviour under aggressive conditions of corrosion, and their modeled thermodynamic stability, yields a sound composite picture of these materials, as schematised in Figure 2. For conceptual purposes, the "favourable zone", "gray zone" and "less favourable zone" of Figure 2 have not been assigned numerical boundaries, the latter being more a matter of technical and political considerations to be developed as a guideline.

FIGURE 2

The three key parameters, physico-chemical characteristics, dynamic behaviour and thermodynamic durability, defining the composite picture of HT materials are discussed below. On the basis of the knowledge acquired over decades on nuclear high level waste glasses (Bates *et al.*, 1994; Ewing, 1996; Thomassin, 1995, 1996; Vernaz and Dussosoy, 1992), these key parameters may drastically influence the long-term durability of our HT materials.

For an accurate description of the experimental setup, the analytical procedure, and the detailed characteristics of each of the individual 23 HT materials studied, the reader should refer to Perret *et al.* (2000, 2002, 2003).

2.1 PHYSICO-CHEMICAL CHARACTERISTICS OF HT MATERIALS

The 23 HT materials studied were produced from Swiss, German, French and Italian HT treatment technologies which were fed by different input materials under realistic conditions of operation (*i.e.* wastes and residues representative of average MSW, BA, FA and FC). These technologies can be roughly grouped into two categories (see Figure 3), in-line processes and post-processes:

1. In-line processes are technologies which directly inertise municipal solid wastes. Five such HT materials were obtained from four different processes. Extrapolated to the entirety of the Swiss MSW, these processes would be fed by *ca.* 3×10^6 t MSW/yr.
2. Post-processes, which inertise the residues of conventional MSW incinerators, can be further grouped into two sub-categories:
   - Post-processes for bottom ash, which are fed by bottom ash (BA; 80-100%, either in rough or fine fractions) and up to 20% fly ash (FA). Six such HT materials were obtained from five different processes, which would have to transform the equivalent of *ca.* 750×10^3 t/yr BA (or *ca.* 248×10^3 t/yr BA in their fine fraction), and up to *ca.* 46.5×10^3 t/yr FA, if extrapolated at the scale of the Swiss residues.
   - Post-processes for fly ash, which are fed by fly ash (FA; 50-100%) and up to 50% of other waste material (filter cake, sewage sludge, cement, recycled glass, or even car shred). Twelve such HT materials were studied; they were produced by nine different technologies, which would be fed by *ca.* 46.5×10^3 t/yr FA, eventually complemented by up to *ca.* 11.625×10^3 t/yr FC or other waste materials.

The factor governing the final size and morphology (from millimeter-sized grains or granules to thin or thick plates and regularly shaped beads, and to medium or large irregular blocks) of HT materials is the quenching technique used in the different HT treatment technologies for the cooling down of the melt.

FIGURE 3

One non-radioactive surrogate (SON68) of the French nuclear high-level waste (HLW) borosilicate glass R7T7 was added to the set of samples as an analytical standard; this HT material is one of the most studied HLW glasses (Nogues, 1984; Fillet, 1987; Advocat, 1991; Cheron *et al.*, 1995). Two other well defined French HT materials (R2bis; R3) produced from FA were also used as analogues of the 23 HT samples for comparative purposes, as their composition and behaviour have been thoroughly studied (Colombel, 1996; Colombel *et al.*, 1997).

Intuitively, the characteristics and behaviour of HT materials would be expected to strongly rely on the operating characteristics of the thermal treatment technologies (e.g. type of combustion chamber, melting temperature) and on the feeding material (e.g. MSW, BA, FA, with other additives). In some cases (*e.g.* the proportion of more volatile to less volatile elements in the HT material), rough trends were indeed observed. However and surprisingly, the vast majority of results did not exhibit clear differenciations on the exclusive basis of the types of HT processes or input wastes and residues, even for samples with highly contrasted macroscopic and microscopic features (see Figure 4).

FIGURE 4

The majority of samples (15 out of 23) were shown to contain no or less than 2% of crystalline inclusions and have a low specific surface area (S_{spec} = 300-600cm^2/g for material ground to 100-125μm); these samples are considered as vitreous. The remaining others contain negligible amounts of crystalline components, either homogeneously or heterogeneously dispersed in a vitreous matrix; they are considered as vitrocrystalline (labelled with an asterisk) and are expected to exhibit a lower durability because of their higher specific surface area (S_{spec} = 400-1000cm^2/g, with 3 exceptions at S_{spec} = 3600-8200cm^2/g). None of the HT materials studied exhibited purely crystalline characteristics.

X-ray diffractograms (see Figure 5) and petrographic analyses (Scanning Electron Microscopy; also used for estimating the surface roughness and micro-heterogeneity of samples) indicate the presence of diverse silicates and oxides on the surface and in the bulk of the vitrocrystalline samples; in addition to the quasi-ubiquitous presence of quartz, other minerals were found from sample to sample: gehlenite, albite, diopside, portlandite, pyroxenes and spinels, but also alloys, plagioclase and metallic inclusions. The presence of crystalline phases in the vitreous matrix of HT materials is explained both in terms of quenching ratea (slow cooling favours the build up of crystals) and embedding of relicts inherited from the input material. Many crystalline phases identified were enriched in trace metals, in particular chromium, copper and zinc dominating most HT samples.

FIGURE 5

Although the role of crystalline phases in the leacheability of HT materials is unclear and must be examined from case to case, the identified silicates and oxides are globally more resistant to corrosion than silicate glass and residues of incineration (BA, FA, FC). Thus, a clear assessment of the durability of HT materials as a function of crystalline components must take into account the combined effects of their enrichement or depletion in trace metals, their individual leachability, the increase (but sometimes decrease) in overall reactivity due to local heterogeneities and increased S_{spec} (Adams, 1992; Bickford and Jantzen, 1984; Jantzen *et al*., 1984; Scholze, 1991; Sproull *et al*., 1994; Sterpenich, 1998).

Probably the most important factor affecting the long-term stability of waste glasses is their composition (Gutman, 1996; Scholze, 1991). Glass is a non-stoichiometric, aperiodic, amorphous and quasi homogeneous solid, which can accept a wide range of waste compositions and concentrations in its matrix (Dietzel, 1988; O'Keefe, 1984; Zachariasen, 1932). Due to its nature, glass is not in equilibrium with its environment and tends to transform into more stable phases. Glass is a three-dimensional unordered arrangement of orthosilicate tetrahedra ($H_2SiO_4^{2-}$) linked together by siloxane oxygen atoms (Si-O-Si) into a network of polymeric chains (-[H_2SiO_3]-[H_2SiO_3]-) (Zachariasen, 1932; Stanworth, 1950). Terminal silanol groups (Si-OH) host protons, alkali elements (Na^+, K^+, Li^+) and alkaline earths (Ca^{2+}, Mg^{2+}), while elements with higher charge (Al^{3+}, Fe^{3+}, B^{3+}, Zr^{4+}, Mn^{4+}) replace Si^{4+} into the glass matrix, acting as network-forming elements or network-modifying elements (Darab *et al*., 1996). Roughly, terminal elements decrease the stability of the glass, as opposed to matrix elements. The proportion of the network-forming element silicon will directly influence the homogeneity of the glassy matrix of HT materials, and thus their durability. On the other hand, the proportion of the network-modifying element calcium will impair the stability of the matrix. Alternatively, elements like aluminum may act either as beneficial network-forming elements (in tetrahedral sites) or as detrimental network-modifying elements (in octahedral sites).

Taken as a whole (see Figure 6), HT materials contain high proportions of silicon ([SiO_2] = 41%, ranging from an average 36.8% for FA-derived HT materials to an average 48.2% for BA-derived HT materials) and aluminum ([Al_2O_3] = 16.5%, ranging from 14.5% for MSW-derived samples to 18.1% for FA-derived samples), while their calcium content may be important ([CaO] = 23.1%, from 17.5% for BA-derived samples to 27.5% for FA-derived samples). It must be highlighted that HT materials prepared from fly ash (and eventual additives) are in average the poorest in Si and the richest in Ca (SiO_2 and CaO being inversely correlated); they would be expected to exhibit a lower durability upon corroding conditions. Nevertheless, the amount of Si and Al in samples is high ([SiO_2 + Al_2O_3] = 45-75%), whatever their origin, suggesting that HT materials should behave globally in a favourable way when subjected to leaching, as opposed to the conventional residues (BA, FA, FC) of low temperature incineration. In addition, the ratio [SiO_2]:[CaO], which gives a rough indication of the expected stability of HT materials, is systematically above 1, though lower for FA-derived materials (in-line processes: 2.94; post-processes for BA: 2.92; post-processes for FA: 1.4).

When expressed as ternary SiO_2 - Al_2O_3 - CaO materials, HT samples remarquably belong to the domain of compositions that form silicate structures (Perret *et al.*, 2000, 2002), vitrocrystalline samples having a high S_{spec}, a rough surface, or many mineral inclusions being roughly in the Si-poor range of compositions.

FIGURE 6

The minor constituents magnesium, sodium, potassium and iron are present in HT materials in highly variable proportions ([MgO + Na_2O + K_2O + Fe_2O_3] = 6-25%). Amongst these constituents, the alkali elements are known to favour phase-separated glasses impairing resistance to leaching (Scholze, 1991; Stanworth, 1950), but their low proportion in the studied samples ([Na_2O + K_2O] < 7%) should not drastically influence the long-term stability of HT materials.

When dealing with potential secondary raw materials with respect to environmental impacts, one has to keep in mind that their content in toxic trace metals should be as close as possible to primary raw materials, though a high metal concentration does not necessarily translate into important releases during leaching. In our case, HT treatment technologies are shown to efficiently scavenge and embed high proportions of metals in the matrix of their

corresponding HT materials (see Figure 7). As expected FA-derived HT materials exhibit higher concentrations of the most volatile elements cadmium, lead, antimony than MSW- or BA-derived HT materials, in agreement with the known accumulation of these metals in fly ash and depletion from bottom ash during conventional incineration.

FIGURE 7

When comparing HT materials to the Swiss guidelines for wastes and residues (TVA, Technische Verordnung über Abfälle; BUWAL, 1996), it appears that only 8 samples out of 23 could be disposed off into landfills for inert materials, on the exclusive basis of their proportions of toxic trace metals ([Cd]: max. 10mg/kg; [Cu], [Ni], [Pb]: max. 500mg/kg; [Zn]: max. 1000mg/kg; the other metals are not regulated with respect to admissibility in landfills). The other HT materials contain between one and five metals that may exceed up to 27× the trigger value of the Swiss guidelines, and would thus require special post-stabilisation prior to landfilling. However, the Swiss guidelines were designed to discriminate the conventional residues (BA, FA, FC) of low temperature incinerator, which are known to have a poor durability with respect to leaching (ABB-EAWAG-EMPA-KEZO, 1990; BUWAL, 1998; EKESA, 1992). Thus, it would be false to assess the critical sustainability of secondary raw materials on the exclusive basis of their metal content, without determining their behaviour upon corrosion.

Figure 8 is an attempt to summarise and group all observations on the physico-chemical characteristics of HT materials (macroscopic, microscopic and physical features, chemical composition, metal content). This figure highlights samples which globally present highly favourable characteristics, and on the opposite those which exhibit no favourable picture. The gauge for categorising HT samples as having only few crystalline inclusions, with a small specific surface area and a smooth surface is the surrogate of the French HLW glass R7T7. The vitreous and homogeneous state of HT samples is based on semi-quantitative measurements by X-ray diffraction and electron microscopy. Finally, the scale for ranking HT samples with respect to their metal content is the Swiss guideline for wastes and residues, though it may not be considered as fully relevant in the case of HT materials with an expected long-term durability.

FIGURE 8

Surprisingly, only 3 HT samples, all of them being vitrocrystalline, would be considered as outside the range of favourable HT materials in terms of secondary raw materials. Out of the 20 other samples, 15 exhibit either two or three favourable characteristics, without obvious relationship between the physico-chemical characteristics of HT materials and their parent process or feeding material. Whatsoever, these characteristics must be weighted together with the behaviour of HT material during corrosion, as discussed below, in order to gain a broader and more relevant picture on their long-term durability and potentialities as secondary raw materials.

2.2 DYNAMIC BEHAVIOUR OF HT MATERIALS DURING CORROSION

As glass is a metastable phase in disequilibrium with its environment, it undergoes over time a series of transformations, collectively called corrosion or alteration. Over the past decades, a consensus has emerged on the steps describing glass corrosion (Adams, 1984; Advocat, 1991; Atassi, 1989; Bates *et al.*, 1994, 1996; Clark and Zoitos, 1992; Clark *et al*., 1994; Cunnane and Allison, 1994; Cunnane *et al*., 1993; Dran *et al*., 1989; Ebert and Mazer, 1994; Ewing, 1996; Feng *et al*., 1994; Grauer, 1985; Lutze and Ewing, 1988; Nogues, 1984; Nogues *et al*., 1985; Petit *et al*., 1990; Scholze *et al*., 1982). On the basis of the extensive work on the behaviour of HLW glasses, glass corrosion systematically exhibits a sequence of three reactions summarised below (see Figure 9):

FIGURE 9

1. Initial ion-exchange: Unaltered glass undergoes diffusion of water molecules from its surface to its matrix. Water reacts with terminal alkali elements in a process of ion exchange (Charles, 1958; Garland and White, 1985):

   $\equiv Si\text{-}O\text{-}Alk + H_3O^+ \rightarrow \equiv Si\text{-}O\text{-}H + H_2O + Alk^+$

   This acidic attack consumes H_3O^+ from the surrounding environment (basification) and releases alkali elements from the glass (dealkalinisation). The reaction is kinetically limited by diffusion of water molecules into the bulk of the glass through the gel layer (see below). The thickness of the diffusion (or reaction) layer is around 1-5μm. This step is then followed by:

2. Matrix hydrolysis: Once glass starts to corrode, water molecules react with internal and external siloxane groups in a process of hydrolysis and dissolution (Bates *et al.*, 1991; Carroll *et al.*, 1994; Clark and Zoitos, 1992; Scholze, 1991; Zellmer and White, 1985):

   $\equiv Si\text{-}O\text{-}Si\equiv + OH^- \rightarrow \equiv Si\text{-}O^- + HO\text{-}Si\equiv$ (internal glass hydrolysis)

   $\equiv Si\text{-}O\text{-}Si(OH)_3 + OH^- \rightarrow \equiv Si\text{-}O^- + H_4SiO_4$ (external glass hydrolysis and dissolution)

   This nucleophilic/basic attack consumes OH^- (acidification) and releases silicic acid and other network-forming and network-modifying elements (devitrification). During this alteration step, $\equiv Si\text{-}O^-$ groups being formed are eventually reprotonated by surrounding water molecules. The gel layer, which thickens during hydrolysis and extensive dissolution, is amorphous in nature (Luo *et al*., 1997).

   Indeed, ion exchange (production of OH^- in the reaction layer) and matrix hydrolysis (consumption of OH^- from the reaction layer and the surrounding environment) are intimately coupled, devitrification being autocatalysed by ion exchange and both processes being enhanced by water diffusion (Grambow, 1992). This step is then followed by:

3. Surface precipitation of secondary phases: At longer term, ion exchange and matrix hydrolysis drive to slow pre-concentration and supersaturation of the released species (alkali elements, silicic acid, network-forming and network-modifying elements). Supersaturation occurs into the thick gel layer and eventually in the bulk solution (Bradley and Bates, 1990; Malow, 1982; Petit *et al*., 1990). In addition, ionic species initially present in the leachant may be complexed and adsorbed at the solution-gel interface and eventually increase supersaturation (Grambow, 1985; Strachan *et al.*, 1985; Whitehead *et al*., 1993).

   When supersaturation is reached, secondary phases start to precipitate, mostly at the surface of the altered glass, but also in solution and, to a lesser extent, into the gel layer (Bates *et al*., 1991; Petit *et al*., 1990; Lee and Clark, 1985; Flintoff and Harker, 1985; Haaker *et al*., 1985; Jercinovic *et al*., 1989; Shuttleworth and Monteith, 1997). Secondary phases are thermodynamically more stable than their individual constituents originally embedded in the glass matrix (Feng *et al*., 1994). These precipitates are either amorphous/poorly crystallised or crystalline (Bates *et al*., 1991; Gong *et al*., 1996; Murakami *et al*., 1989). Although some secondary phases are frequently detected (smectites of various composition, zeolites, chrysotile, quartz, kaolinite, illites, spinels, hydrotalcites) at the surface of corroded glasses (Abdelouas *et al*., 1997; Bourcier *et al*., 1989; Bradley and Bates, 1990; Buck *et al*., 1994; Gong *et al*., 1996; Gislason *et al*., 1993; Jercinovic *et al*., 1989; Mottl and Holland, 1978;

Murakami *et al*., 1989), the extremely high diversity of precipitates (which mostly but not exclusively contain matrix elements as oxides, oxyhydroxides, phosphates, carbonates and silicates) reflects the composition of both the glass and the solution chemistry of the leachant (Bart *et al*., 1985; Feng *et al*., 1994; Petit *et al*., 1990; Whitehead *et al*., 1993; Yanagisawa and Sakai, 1988). This ultimate step in glass corrosion is actually very difficult to modelise.

The time scales of these chemical processes are in the order of days to weeks (step 1), weeks to months (step 2), and months to years (step 3). Although the two first steps are well described by refined kinetic and thermodynamic models, the long-term fate of glass constituents cannot be predicted with accuracy, mostly because of the discrepancies between models and experiments on the nature of the secondary phases formed.

A convenient way to estimate the long-term stability of glasses is to bring them under conditions of accelerated corrosion. Many glass corrosion tests have been designed to yield the detailed mechanisms of matrix corrosion and kinetics of glass dissolution. However, it must be stressed that these tests are usually performed under conditions of corrosion far from realistic ones (*e.g.* high temperature, high concentration of leachants, high reactive surfaces, *etc.*), forcing the solid-solution interface far from equilibrium and thus inducing additional uncertainties on the long-term behaviour of glasses. Of course, real time corrosion experiments (*e.g.* burrial of glasses in soils, landfill disposal, reuse in civil engineering applications) are of major interest, but they yield valuable results after decades and they cannot thus be considered as relevant in our case.

For our HT materials, and taking into account their morphological diversity (small grains to large blocks), a dedicated corrosion test was designed, hereafter referred to as the Strasbourg test. The test is performed under static conditions at high temperature (leachant = 50mL H_2O; HT material = 50mg ground to 100-125µm; no stirring; T = 90°C; duration = 1, 3, 10 days), with pH evolving freely during corrosion in the closed vessel. At the end of the experiment, the leachate is analysed for pH and major, minor and trace elements, and the HT material is recovered for microscopic examination.

Figure 10 highlights the transformations induced on the surface structure of HT materials after 10 days corrosion. The amorphous gel layer which appears during corrosion is observed on most HT samples and reveals pits, holes and corrosion paths from case to case. For many samples, crystalline secondary phases cover the altered surface, and spallation of the gel layer is observed in several instances, suggesting that corrosion is a discontinuous process, even under static conditions.

FIGURE 10

From a theoretical point of view, the gel layer is a barrier which reduces further hydrolysis of the silicate network, and is supposed to be more stable than the glass matrix, thus reducing the overall rate of corrosion. However, gel exfoliation may momentarily re-activate corrosion, at least locally. No clear trend rules the presence of the crystalline secondary phases identified at the surface of the corroded HT samples. The most abundant minerals are aluminosilicates, calcium phosphates, iron-rich and magnesium-rich minerals, and zeolites; their role in the scavenging or release of toxic metals remains however ambiguous, although many mineral phases identified bear traces of metals.

In a first quote, matrix dissolution (see Figure 11a), which is approximated as the release of silicon in the solution, is somewhat correlated to the pH of the leachant, indicating that glass dissolution is favoured at higher pH; this feature

is in agreement with the mechanisms of the second step of corrosion (see above). On the other hand pH, which evolves freely during the corrosion experiments, is mostly -but not exclusively- controlled by the release of alkaline species in the leachant, amongst which calcium plays the major role (see Figure 11b); this relationships is fairly tight after 1 day corrosion, but weakens while the pH raise becomes much slower with time, suggesting that the extraction of alkaline elements in the leachant is not a congruent process, and indicating that pH stabilises rapidly during matrix dissolution. In fact, the proportion of calcium in the matrix of HT materials (11-38%) directly governs the amount of calcium which will be readily leached out (see Figure 11b). As a corolary of our observations, Ca-poor/Si-rich HT materials are expected to show a higher durability than Ca-rich/Si-poor ones. The relationship between Ca in the matrix of HT materials, Ca^{2+} extracted in solution by the leachant, and pH is given by:

$$\{CaO\}_{HT\ material} + 2H_2O \rightarrow Ca^{2+} + 2OH^-$$

$$\{CaSiO_3\}_{HT\ material} + 2H_2O \rightarrow Ca^{2+} + H_4SiO_4 + 2OH^-$$

FIGURE 11

Whatever the physico-chemical characteristics of HT materials, the concentrations of most major, minor and trace elements in the leachant increase with time, but stabilise around limiting values (see Figure 12). In addition, the relationship between released concentrations and time of corrosion does not superimpose from sample to sample and from element to element, indicating that matrix dissolution is a complex non-congruent process, which cannot be explained in terms of simple physico-chemical characteristics of the samples. It must indeed be pointed out that the true release of elements, *i.e.* their extraction from the glass matrix, cannot be accessed, because many released elements will be precipitated, or trapped into the gel layer, or scavenged by the secondary minerals (Crovisier *et al.*, 1987, 1992; Grambow, 1994; Malow, 1982; Petit *et al.*, 1990). Thus, the concentrations measured in the leachant are merely apparent releases, which impairs the accurate description of the mechanistics of glass corrosion.

FIGURE 12

Trace elements, as exemplified by the case of Pb on Figure 12, frequently exhibit an increase in concentration between 1 and 3 days of corrosion, followed by a decrease between 3 and 10 days; the extend of the trend varies strongly from sample to sample and from element to element. This observation supports the hypothesis that crystalline secondary phases forming at the surface of corroded HT materials act as trace metal scavengers.

The Strasbourg test is performed under much more drastic conditions of corrosion (finely powdered samples reacted 10 days at high temperature) than the corrosion test described by the Swiss TVA guideline for disposal of residues in landfills for inert materials (coarsely ground samples reacted with CO_2-saturated water during 24h at room temperature; BUWAL, 1990). Nevertheless, we observed that the released toxic metals never reached the maximum trigger concentrations of the TVA guideline: Cr < 40µg/L (TVA_{max} = 50µg/L), Co < 0.4µg/L (TVA_{max} = 50µg/L), Ni < 22µg/L (TVA_{max} = 200µg/L), Cu < 19µg/L (TVA_{max} = 200µg/L), Zn < 113µg/L (TVA_{max} = 1000µg/L), Cd < 2.7µg/L (TVA_{max} = 10µg/L), Sn < 0.7µg/L (TVA_{max} = 200µg/L), Pb < 2.5µg/L (TVA_{max} = 100µg/L). In comparison, bottom ash and fly ash of conventional low temperature incineration usually lead to much higher concentrations of metal, usually exceeding the trigger values, when corroded under the conditions of the Swiss leaching test.

In order to assess, or at least estimate, the long-term durability of HT materials, one needs to express the results of corrosion experiments in terms of apparent normalised release rates of elements (Perret *et al.*, 2003). For comparison purposes (from element to element, and from sample to sample), these rates are normalised with respect

to the characteristics of the HT materials (mass of sample, surface exposed to leachant), the elements of interest (concentration in the sample, apparent concentration released in the leachant), and the experimental conditions (volume of leachant, duration of corrosion). Apparent normalised release rates of elements (i) are expressed as:

$$r(i)_{norm} = d (\{ [C_i]_{leachate} \times V_{leachant} \} / \{ [C_i]_{HT\ material} \times S_{HT\ material} \}) / dt \quad [g/m^2 \times day]$$

FIGURE 13

Figure 13 shows representative examples of apparent release rates of several major (Si, Ca), minor (Na, K) and trace elements (Sn, Pb) of selected samples. Once again, the apparent congruency of the releases is clearly not respected, either from element to element in the same HT material (sample P12.1), or from sample to sample for the same element. This is indeed in agreement with usual observations, showing the complex solution and secondary mineral chemistries (Grambow, 1985 ; Advocat, 1991) Whatsoever, most alkali elements are roughly released at higher rates than network-forming and network-modifying elements, indicating that the latter will be predominantly precipitated as secondary minerals. Apparently, the normalised release rates of major elements seem to be partly influenced by the original type of residues used to produce the HT materials (r{in-line processes} > r{post-processes for FA} > r{post-processes for BA}). On the other hand, trace elements exhibit a broad range of apparent release rates, but their calculation is partly biased by the low concentrations of metals in the HT materials and in the leachants.

The main conclusion that one may draw from the leaching experiments performed under the drastic conditions of the Strasbourg corrosion test is that short-term releases (1 day corrosion) are highly differentiated from sample to sample (highly contrasted apparent normalised release rates) and can be discriminated into fast-reacting and slow-reacting materials. The chemistry of the leachates at the beginning of corrosion is governed by the composition of HT materials, corrosion being primarily controlled by pH, which is in turn equated to the proportion of CaO in HT materials. However, the releases rapidly decrease and converge toward similar limiting values, around $r(i)_{norm}$ = 0.2-0.25$g/m^2 \cdot d$ for major and minor elements, whatever the nature of the HT materials.

In addition, one may notice that, although most HT materials could not be disposed off into landfills for inert materials on the basis of their content in toxic trace metals (see Chapter 2.1 and Figure 7), they all release very small concentrations of these metals during accelerated corrosion experiments, much below the trigger values of the Swiss regulation. This demonstrates that HT materials pre-concentrate fairly large proportions of toxic trace metals in their matrix, and they embed them over the long-term when subjected to corrosion, whatever the technology developed to produce these materials; on this basis, HT materials comply to the conditions required for safe secondary raw materials.

Finally, the apparent normalised release rate of silicon ($r(Si)_{norm}$) of HT samples, which can be approximated as the dissolution rate of the samples, was compared to the one obtained for the standard HLW glass SON68 under the same conditions of corrosion. Out of the 23 HT samples tested, 6 samples (P1, P2*, P4.1*, P6*, P7, P11*) exhibit $r(Si)_{norm} \leq$ SON68, thus presenting a highly favourable dynamic picture with respect to their long-term durability.

FIGURE 14

Figure 14 is a rough comparison of the static and dynamic characteristics of HT materials. This Figure shows that HT materials can be discriminated, but that they collectively exhibit worthy characteristics and behaviour. Note that two samples (P6*, P11*) out of the three most exemplary HT materials (samples at the union of the three domains of high standard of quality) are vitrocrystalline. On the other hand, HT materials P1, P2* and P4.1*, which contain

elevated proportions of toxic metals, would paradoxaly not be allowed into landfills for inert materials, although their reactivity is lower than the one of the standard HLW glass SON68.

2.3 THERMODYNAMIC DURABILITY OF HT MATERIALS

A relevant and quantitative way of combining the physico-chemical characteristics of HT materials and their dynamic behaviour as a consequence of corrosion has been developed by Paul and Newton (Newton, 1985; Newton and Paul, 1980; Paul, 1977, 1982) and refined later by Jantzen and Plodinec (Jantzen, 1984, 1988; Jantzen and Plodinec, 1984; Plodinec, 1984; Plodinec and Wicks, 1994). This model makes use of the thermodynamic assessment of glass hydration to estimate the relative stability of glasses, and has been used successfully to predict the long-term stability of nuclear HLW glasses (Bates *et al.*, 1994; Ewing, 1996; Sproull *et al.*, 1994). The assessment requires the determination of the overall free energy of hydration ΔG_{hydr} of the glass, which is estimated as the molar-weighted sum of the free energies of hydration $\Delta G_{hydr}(i)$ of its individual constituents:

$\Delta G_{hydr} = \Sigma(X_i \times \Delta G_{hydr}(i))$

X_i = molar fraction of the constituent (i) in the glass; X_i are obtained from the chemical analysis of the glass.

$\Delta G_{hydr}(i)$ = free energy of hydration of the individual constituents (i) in the glass; $\Delta G_{hydr}(i)$ values are available in the literature for most silicates and oxides, or calculated as $\Delta G_{hydr}(i) = -RT \times \ln(K_{hydr}(i))$.

The model assumes that glass is an homogeneous 3-dimensional network of tetrahedrons MO_4^{4-} (M = network-forming elements Si, Al, B), with network-modifying elements (Ca, Mg, Na, K, Fe) and trace elements being dissolved into the network. According to the model, the assembly will hydrate spontaneously upon corrosion in a congruent manner, assuming that no secondary minerals form at the surface of the corroded glass. Negative values of ΔG_{hydr} correspond to materials that hydrate more spontaneously, *i.e.* that dissolve easily in water (see Figure 15 below).

To complete the thermodynamic approach, it has been observed that there exists a fairly tight relationship between the calculated ΔG_{hydr} of a glass, and its apparent normalised release rate, as determined during accelerated corrosion tests (Plodinec and Wicks, 1994); this relationship has been verified on a large palette of glasses of different origins (HLW, natural, ancient and commercial glasses). The complete thermodynamic approach thus consists in estimating the durability of a glass on the basis of its thermodynamic propensity to corrode and to relate this durability to the experimental release rate of the glass.

Although the thermodynamic model should in principle be used exclusively for glasses, we applied the concept to our set of vitreous and vitrocrystalline HT materials, considering that the minute amounts of crystalline components present in the vitrocrystalline samples would not drastically impair the determination of their overall free energy of hydration. In addition, trace elements, for which hydration data are either unknown or inaccurate, were not included in the calculation of ΔG_{hydr}, except for Ba, Zn, Zr (known thermodynamics; non negligible concentrations in some samples); the error in ΔG_{hydr} caused by the missing contribution of trace elements should be negligible, except for Cr (up to 7500 mg/kg) and Cu (up to 2500 mg/kg) in some samples. The model used for the computation of ΔG_{hydr} and the specific processing pertaining to our HT materials are detailed and discussed elsewhere (Advocat, 1991; Linard, 2000; Perret *et al*., 2000, 2003).

FIGURE 15

Figure 15 is a composite diagram showing the evolution of the calculated free energy of hydration of our HT materials over a wide range of pH. The curves obtained for all samples originating from the same family of HT treatment technologies (in-line processes for MSW wastes; post-processes for BA, post-processes for FA) have been grouped, for simplicity, into individual domains of stabilities (shaded areas).

For clarity, the schematic evolution of ΔG_{hydr} of two hypothetical glasses subjected to corrosion, one SiO_2-rich/CaO-poor (upper curve) and one SiO_2-poor/CaO-rich (lower curve), is overlaid on Figure 15. The Si-rich glass exhibits a higher stability than the Ca-rich glass. For the former, the curve is steeper at higher pH, indicating that SiO_2-rich glasses hydrate more spontaneously in alkaline solutions; on the opposite, CaO-rich glasses (steeper solpe at lower pH) dissolve more easily under acidic conditions.

While the pH measured after 1-10 days corrosion under the conditions of the Strasbourg test ranged from 7 to 10.3, the individual curves $\Delta G_{hydr} = f(pH)$ of HT materials indicate that their maximum thermodynamic stability would be reached around pH = 5-7.5. Taken collectively, HT materials originating from in-line processes are spread over a wide range of ΔG_{hydr} values (ΔG_{hydr} = -4.7kcal/mol ± 3.1); this is indeed explained by the fact that the composition in major and minor species in these samples has a large variability (see standard deviations on Figure 6). On the other hand, HT materials produced by post-processes for BA present a narrower band of stabilities (ΔG_{hydr} = -5.0 kcal/mol ± 1.5), in agreement with their rather homogeneous sample-to-sample composition. Finally, post-processes for FA yield HT materials which are collectively less stable (ΔG_{hydr} = -9.6kcal/mol ± 2.0) than the others, as a consequence of the enrichment of fly ashes in CaO with respect to SiO_2 (see Figure 6).

Whatsoever, HT materials exhibit alltogether stabilities around the one of the standard HLW glass SON68, designed to be highly durable; this is indeed a highly favourable feature of the predicted long-term stability of HT materials. The overall free energy of hydration of HT materials is primarily governed by those components present in large proportions and exhibiting large $\Delta G_{hydr}(i)$ values. As expected, samples containing high amounts of network-forming components (SiO_2, Al_2O_3, Fe_2O_3 and in particular MnO_2) and low amounts of network-modifying components ($CaSiO_3$ and to a lesser extent Na_2SiO_3 and $MgSiO_3$) are characterised by the highest thermodynamic stabilities.

An extended survey of the relationship between calculated free energies of hydration ΔG_{hydr} and experimental apparent normalised release rates $r(i)_{norm}$ is presented in Figure 16 (Plodinec and Wicks, 1994) for a series of 115 glasses of different origins. The empirical relationship was obtained by means of the MCC-1 test (Bates *et al.*, 1994; Ebert and Mazer, 1994). The MCC-1 test is an accelerated static corrosion test performed on glass cubes in water, at 90 °C during 28 days; it was designed to assess the reactivity of nuclear HLW glasses to be stored in deep geological repositories.

FIGURE 16

Because of technical constraints (several HT samples cannot be cut into $4cm^2$ monoliths, because of their granular nature), the MCC-1 test could not be performed with our set of samples. Nevertheless, the normalised apparent dissolution rates of HT materials ($r(glass)_{norm}$), approximated as the release rates of silicon ($r(Si)_{norm}$) obtained by the Strasbourg test (100-125μm powdered samples), have been overlaid on Figure 16 for comparative purposes; for

simplicity, the results obtained after 3 days corrosion are ommited. Although not perfectly similar, the MCC-1 test and the Strasbourg test can at least be related in terms of their matching efficiencies ($S_{HT\ material}/V_{leachant})\times t_{corrosion}$ = 2.8day/cm for the MCC-1 test; 0.2-2day/cm for the Strasbourg test).

Figure 16 shows that the ΔG_{hydr} *vs.* $r(i)_{norm}$ relationship for HT materials corroded during 1 day is very close to the one obtained on various glasses by the MCC-1 test; in addition, the standard HLW glass SON68 (Strasbourg test) yields similar results to the ones obtained for the other nuclear HLW glasses (MCC-1 test), confirming that both tests can be compared, at least for the initial stage of corrosion of the Strasbourg test. Although based on simplifying assumptions, the thermodynamic approach of the free energy of hydration can clearly be applied to discriminate HT materials during the initial stage of matrix hydrolysis: A difference of 10 kcal/mole between two HT samples yields an approximate one order of magnitude difference between their dissolution rates.

It has already been observed that normalised apparent release rates of major and minor elements present in HT materials converge toward similar values on longer terms of corrosion (*ca.* 0.2-0.25g/m^2·day; see Figure 13). This is confirmed on Figure 16, where the influence of the differences in ΔG_{hydr} on the release rates vanishes for 10 days leaching (quasi-flat slope). This indicates that the corrosion of HT materials is highly contrasted during the initial stages of dissolution, but rapidly shifts towards uniform behaviours representative of a regime of quasi-equilibrium, most probably as a consequence of the protective effect of secondary minerals formed at the surface of corroded HT samples. In addition, medieval glasses (MCC-1 test) and our HT materials (Strasbourg test; 10 days corrosion) exhibit similar slopes, which may be explained by the formation of protective Mg-rich phases in both cases (Crovisier *et al.*, 1987; Abdelouas *et al.*, 1997).

On the basis of our results and the ones obtained by the MCC-1 test, the durability of our HT materials is estimated to range between 10^3 years and 10^4 years. By comparison, medieval and antique glasses have an observed durability above 10^3 years (Gillies and Cox, 1988; Macquet and Thomassin, 1992; Stepenich, 1998), while the extrapolated durability of nuclear HLW glasses extends above 10^4 years (Jollivet *et al.*, 1998).

3. "GLASSFILL" VERSUS "GLASSROAD"

The description of HT materials by means of their physico-chemical and microscopic characteristics (static features; see Chapter 2.1), their behaviour under aggressive conditions of accelerated corrosion (dynamic features; see Chapter 2.2), and their estimated thermodynamic stability (thermodynamic features; see Chapter 2.1) helps us to derive a composite, yet semi-quantitative picture of the individual qualities of HT materials from the point of view of the energy-to-waste-to-environment path. This is the aim of Figure 17, where each HT material has been assigned a relative rank with respect to its static features (crystallinity, S_{spec}, surface roughness, density of mineral inclusions, amount of metals), dynamic features (Si loss in the leachate, normalised apparent release rate), and thermodynamic features (free energy of hydration). The combination of each of these features yields an average global rank; details on the computing of the individual ranks are given in Perret *et al*. (2000). In Figure 17, a distinction is made between fully characterised and partly characterised (*i.e.* samples for which several parameters were not determined) HT materials.

FIGURE 17

The gray zone in Figure 17 encompasses the average (± standard deviation) rank for all samples which were fully characterised. The standard HLW glass SON68 and the two standard HT materials R2bis and R3 are shown for comparative purposes. Several HT samples which were not fully characterised (P4.1*, P4.2, P9.2, P12.3*, R3) can be described as globally favourable materials (*i.e.* they lay within the gray zone), while several fully characterised HT samples (P13, P16*) lay below the gray zone. No conclusion can however be drawn for the incompletely characterised HT samples which lay below the gray zone (P3*, P10, P12.2, P17, P18, R2bis), because their final rank is probably underestimated.

Taken collectively, HT materials exhibit globally favourable qualities, and can thus be considered as potential candidates either for disposal into specific landfills for inert-type HT materials requiring no special attention ("glassfill" scenario), or for re-use in civil engineering applications ("glassroad" scenario). The "glassfill" *vs*. "glassroad" approach is based on the following considerations, assumptions, and boundary conditions (for details, see Perret *et al.*, 2000):

- The 28 existing Swiss MSW incineration plants would be either replaced by in-line processes for MSW, or updated with post-processes for BA or FA. These plants would treat 3×10^6t/yr MSW, or 7.75×10^5t/yr BA, or 4.65×10^4t/yr FA, or combinations of them (see Figure 3).
- The annual production of HT materials depends on the type of HT technologies. Taking into account the highest input→output mass transfer coefficient of each process, the following masses of HT materials would theoretically be produced:
  In-line processes: $400\text{-}700\times10^3$t/yr.
  Post-processes for BA: $200\text{-}700\times10^3$t/yr.
  Post-processes for FA: $30\text{-}50\times10^3$t/yr.
  For our "glassfill" *vs.* "glassroad" scenario, it is assumed that the annual production of HT materials in Switzerland would range $50\text{-}700\times10^3$t/yr.
- The composition of HT materials can be approximated as the average composition of all HT materials tested in this study, taking into account the lower and upper concentrations of major, minor and trace elements determined for each of the three families of HT processes. The composition of such a hypothetical HT material is given in Table 1.
- HT materials produced by these HT technologies would be either disposed off into thick "glassfills", or re-used as thin foundation layers for "glassroad" construction. The characteristics of such hypothetical "glassfills" and "glassroads", which depend on the annual production of HT materials, are given in Table 2.
- The resulting "glassfills" and "glassroads" would be exposed to realistic conditions of corrosion. Taking into account the results of the present study and the corrosion rates given in the literature, ranging between 10^{-4} and $2\text{g/m}^2\times\text{day}$ for accelerated corrosion tests (see Perret et al., 2000), the most realistic dissolution rate pertaining to the "glassfill" and the "glassroad" scenarii is $r_{corrosion} = 10^{-4}\text{-}10^{-3}\text{g/m}^2\times\text{day}$.
- The toxic metals released from the "glassfills" and the "glassroads" during corrosion would be dispersed in the environment without special attention. In this way, released concentrations and loads of toxic metals can be compared with fluxes resulting from natural mechanisms and anthropogenic activities.

TABLE 1

TABLE 2

For the case of the "glassfill", the annual production of HT material would result in the opening of a landfill with the dimensions $50\times50m^2$ to $190\times190m^2$ (typical depth of 10m). For the case of the "glassroad", an annual production of $50\text{-}700\times10^3$t of HT material would be equivalent to the construction of ca. 5-70km/yr of a road with the dimensions of a highway (*ca*. 10m width; typical thickness of 50cm).

Because of their specific characteristics (different dimensions and permeabilities), the "glassfill" would drain annually an equivalent $2.6\text{-}37\times10^3m^3$ water, while the "glassroad" would drain annually an equivalent $3.8\text{-}53\times10^3m^3$ water. Thus, the scenario shall consider that a global volume of water comprised between $3\times10^3m^3$/yr and $50\times10^3m^3$/yr would percolate through the pile of HT material, whatever its final destination. This is an important issue on the plausible destination of HT materials, as the investment in energy which is required in their production would generate a much more cost-effective return in the case of the "glassroad" scenario (higher value) than in the case of the "glassfill".

3.1 ESTIMATED IMPACT OF "GLASSFILL" AND "GLASSROAD" ON THE ENVIRONMENT

The model designed to account for all considerations discussed above expresses the releases of toxic metals in terms of concentrations (*i.e*. concentrations of metals released during corrosion of the "glassfill" or "glassroad") and in terms of annual loads (*i.e*. masses of metals released annually). The annual loads of metals released in the environment are computed according to the following expression:

$$m(M^{n+}_{released}) = [M^{n+}]_{HT\ material} \times r_{corrosion} \times ((m_{HT\ material} / \rho_{HT\ material}) / V_{grain}) \times S_{grain} \times \Delta t_{corrosion} \quad [kg/yr]$$

Figure 18 shows the relevant results obtained with the corrosion model.

FIGURE 18

The concentrations and annual masses of metals that would be released in the environment are linearly related to the proportions of these metals in the HT material and to the corrosion rate. However, the released concentrations of metals are independent of the mass of HT material produced annually, while the released annual masses are indeed linked to the annual production. On the other hand, the size of HT granules has a strong influence on the concentrations and masses of metals that would be released, as $m_{released} = f(1/size)$; in other words, a 1mm granule shall release 50× more metal than a 5cm block.

Taking into consideration the upper limits of the scenarii ($[metal]_{HT\ material}$ = 5000mg/kg; granule diameter = 1mm; $r_{corrosion} = 10^{-3}g/m^2\times$day; annual production = 700kt/yr), the maximum concentration of metal released in the environment would be in the order of 80mg/L, for a maximum load of *ca.* 3t/yr. On the opposite (*i.e*. within the lower limits of the scenarii), the minimum concentration of metal released would be in the order of 2ng/L, for a mimimum load of *ca*. 10mg/yr. Table 3 summarises the concentrations and loads which would be expected within the boundaries of the scenarii, for grain sizes of 1cm, which is a realistic size according to the actual morphologies of our set of HT samples, and taking into account the actual average concentrations of metals in our hypothetical HT material.

TABLE 3

The proposed corrosion model allows one to estimate the maximum lifetime of our hypothetical average HT material subjected to realistic conditions of corrosion. The maximum lifetime represents the time necessary to corrode the total amount of HT material, provided that all elements are released at the same rate (*i.e*. congruent mechanism of dissolution) and that the rate is constant throughout the life of the HT material. Table 4 summarises the plausible lifetimes calculated from the different scenarii.

TABLE 4

Within realistic conditions of operation, the shortest lifetime (1200yr) represents the worst case, which is certainly difficult to envision: For this situation, HT granules would have the smallest possible size (1mm) and would dissolve at the fastest rate (10^{-3}g/m^2×day). Likewise, the longest lifetime (6×10^5yr) is the best case which might certainly never happen: HT granules would have the largest size and dissolve at the smallest corrosion rate. These two extreme lifetimes are thus not considered as plausible. For the most realistic estimates, one would expect the hypothetical HT material to last over *ca*. 10^4-10^5 years, which is remarquably positive.

3.2 OTHER NATURAL AND ANTHROPOGENIC FLUXES OF METALS

The relative impact of our hypothetical average HT material on the environment can be compared to other natural and anthropogenic sources of toxic metals.

TABLE 5

Table 5 compares the average concentrations of metals in several materials of natural and anthropogenic origins.As expected from the operating conditions of the various HT treatment technologies, the concentration of chromium in HT materials (*i.e*. in our hypothetical average HT material; see Table 1) is much higher than in the other materials of Table 5, although the continental crust may contain up to 3g/kg of this element. Nickel in HT materials is much below the trigger value for disposal off of residues in landfills for inert materials, and even below the Swiss T value (tolerable concentration in excavation material used for civil engineering purposes). Copper, zinc, cadmium and lead are less concentrated in HT materials than in the conventional residues of incineration (BA, FA, FC); except for lead, these metals exceed the trigger value of the Swiss guidelines for inert landfills.

TABLE 6

Table 6 lists the annual masses of metals immobilised in several anthropogenic materials. Data of Table 6 take into account the concentrations of metals in these materials (see Table 5) and the claimed annual production of these materials in Switzerland. For the case of our hypothetical HT material, two scenarii are taken into account: It is assumed here that the annual production of HT materials would be either 7×10^5t/yr (replacement of the 28 Swiss incineration plants by in-line processes for MSW to treat 3×10^6t/yr of MSW, or update with alternative post-processes for BA), or 5×10^4t/yr (update of the 28 plants with alternative post-processes for FA).

Depending on the type of HT process chosen, the annual mass of metals immobilised in the hypothetical average HT material would either be in the medium-to-high range, or in the low range, of masses of metals in materials produced by human activities. Chromium is indeed an exception, as a consequence of the abundant release of this element from the refractory materials used in most HT technologies. For the other metals, HT materials result in lower annual masses of metals immobilised than MSW and BA produced by conventional incineration; this reflects

satisfactorily that HT technologies are effectively able to separate a pool of recyclable metals which will not end up in the HT material. Whatsoever, the annual masses of metals which would be immobilised in HT materials are in the order of magnitude of the ones immobilised in the Swiss Portland cement.

TABLE 7

Finally, Table 7 compares the extent of several net losses of metals in the environment as a result of (i) the corrosion of our hypothetical HT material, (ii) the anthropogenic dispersion of metal-containing materials used as fertilisers on Swiss soils, and (iii) the masses of metals transported annually by the two major Swiss rivers. Indeed, only sewage sludges falling within the Swiss guidelines for use as fertilisers are considered in Table 7. In the case of HT materials, two boundary conditions are presented: The most conservative case considers an annual production of 7×10^5t HT materials being corroded at the highest plausible rate ($r_{corrosion} = 10^{-3}g/m^2\times day$), while the second case is computed with an annual production of 5×10^4t HT materials being corroded at the lowest plausible rate ($r_{corrosion} = 10^{-4}g/m^2\times day$). Data are also presented as surface-weighted losses of metals, i.e. masses of metals released per square kilometer of soil (use of fertiliser) or "glassfill"/"glassroad"; this distinction is necessary because, for a given mass of HT material, the upper surface of the "glassfill" exposed to rain is smaller than its equivalent "glassroad", as a result of their different thickness (see Table 2).

Table 7 shows that the total mass of metals that would be released by our hypothetical average HT material is by far much smaller (Σ(metals) = 2-400kg/yr, depending on the scenario chosen) than the total mass of metals deposited every year in Switzerland as a result of intensive use of fertilisers (Σ(metals) = 10^6kg/yr for all types of fertilisers). Likewise, the total loadings resulting from corrosion of the HT material is much smaller than the total masses of metals circulating via the Rhine and the Rhône Rivers (Σ(metals) = 10^6kg/yr).

Surface-weighted data, which are more representative of short-range contaminations, indicate that the "glassfill" scenario is much more detrimental to the environment than every other case. The hypothetical "glassroad" would, on the contrary, be less detrimental to soils and natural waters than the use of fertilisers on soils.

In terms of loadings, it is instructive to note that the Rhine and the Rhône Rivers transport annually *ca*. 2.5×10^3 to $10^5\times$ more metals than the ones which would be released during the corrosion of our hypothetical average HT material. Likewise, it appears that the Swiss soils collect annually huge amounts of metals as a consequence of agricultural activities and use of different types of fertilisers.

To conclude, it must be pointed out that the releases of toxic metals in the "glassfill"/"glassroad" scenarii, although realistic, do not take into account the complex mechanisms of immobilisation of metals by precipitation of stable solid phases, either at the surface of the corroded HT material or in solution. These mechanisms of immobilisation are difficult to modelise, but they would in any case decrease the metal concentrations and loadings resulting from the corrosion of the HT materials.

4. A CONCLUDING REMARK

The determination of the global picture of HT materials, by a combination of physico-chemical and microscopic analyses, accelerated corrosion experiments performed under aggressive conditions, and computed spontaneity to hydrate, is a fairly simple comparative tool which allows us to estimate their relative stability.

The key results of this study show that the high-temperature technologies (in-line processes; post-processes) used to produce HT materials, or the original wastes (MSW, BA, FA, FC) used to produce HT materials, have only little influence on the final characteristics and behaviour of these materials. Taken alltogether, HT materials have fairly favourable characteristics and behave on good terms when subjected to corrosion. HT materials may contain up to ca. 10-200× more metals than some anthropogenic and natural materials (cement, clinker, continental crust, granites), but they are globally much cleaner than other residues resulting from human activities (bottom ash, fly ash, filter cake, car shred, sewage sludge). According to the Swiss guidelines, most HT materials cannot be considered as inert materials and could not be disposed off in landfills without requiring pre-stabilisation; however, HT materials release only negligible concentrations of toxic metals under drastic conditions of corrosion, much below the Swiss trigger values used to assess the chemical stability of wastes and residues. When gauged against other analog materials (glasses of different origins), the durability of HT materials, estimated to range between 10^4 and 10^5 years under realistic conditions of corrosion, is exceptionally high.

As a consequence, the production of HT materials and their potential re-use as foundation layers for road construction, or their immobilisation into specific landfills requiring minimal care, would appear globally as a non detrimental activity for our environment, in comparison with other natural and anthropogenic systems.

ACKNOWLEDGEMENTS

The model for the calculation of the free energy of hydration was provided by Dr Thierry Advocat, CEA Marcoule (France). The financial support to D. Perret, P. Stille, G. Shields and U. Mäder was provided by the Swiss Office for the Environment, Forests and Landscape. The financial support to J.-L. Crovisier was provided by the EOST/CGS contribution #2002.408-UMR7517.

REFERENCES

ABB-EAWAG-EMPA-KEZO (1990). Durchführung von Pilotversuchen zur Aufbereitung und Entsorgung von Filterstaub aus Kehrichtverbrennungsanlagen; Schlussbericht. Baden/Dübendorf, Switzerland.

Abdelouas A., Crovisier J.-L., Lutze W., Grambow B., Dran J.-C., Müller R. (1997). Surface layers on a borosilicate nuclear waste glass corroded in $MgCl_2$ solution. J. Nucl. Mat. 240, 100-.

Adams P.B. (1992). Predicting corrosion. In: Corrosion of Glass, Ceramics and Ceramic Superconductors; Principles, Testing, Characterization and Applications (Clark D.E., Zoitos B.K., eds.). Noyes, Park Ridge, U.S.A., 29-.

Advocat T. (1991). Les mécanismes de corrosion en phase aqueuse du verre nucléaire R7T7; approche expérimentale, essai de modélisation thermodynamique et cinétique. PhD dissertation, University Louis Pasteur, Strasbourg, France.

Atassi H. (1989). Evaluation de la résistance à la corrosion en solution aqueuse de quelques verres silicatés. PhD dissertation, University Louis Pasteur, Strasbourg, France.

Barin O. (1991).Behandlungsverfahren zur Inertisierung der Flug- und Filterstäube aus der Müllverbrennung. I. Verfestigungs-, physikalisch-chemische, Keramisierungs-, Zementherstellungs-, Feuerungs- und Brennkammerverfahren. Wissenschaft Umwelt 3-4, 159-.

Barin O. (1992). Behandlungsverfahren zur Inertisierung der Flug- und Filterstäube aus der Müllverbrennung. II. Eelktrothermische Verfahren und Diskussion. Wissenschaft Umwelt 1, 93-.

Bart G., Aerne E.T., Grauer R., Linder H., Z'Berg D., Zwicky H.U. (1985). Surface film characterization of corroded HLW glass specimens.

Bates J.K., Ebert W.L., Mazer J.J., Bradley J.P., Bradley C.R., Dietz N.L. (1991). The role of surface layers in glass leaching performance. Mat. Res. Soc. Symp. Proc. 212, 77-.

Bates J.K., Bradley C.R., Buck E.C., Cunnane J.C., Ebert W.L., Feng X., Mazer J.J., Wronkiewicz D.J., Sproull J., Bourcier W.L., McGrail B.P., Altenhofen M.K. (1994). High-level waste borosilicate glass: A compendium of corrosion characteristics. Technical report DOE-EM-0177, US-DOE, Washington, USA.

Bickford D.F., Jantzen C.M. (1984). Devitrification behavior of SRL defense waste glass. Mat. Res. Soc. Symp. Proc. 26, 557-.

Bottero J.Y., Chatelet L., Leforestier L., Sterpenich J., Libourel G., Brown W., Yvon J., Bigois M. Remontet S., Olle M., Mosnier F., Bouchelaghem A. (1997). Les déchets ultimes inertes peuvent-ils devenir des matériaux utiles? Proc. Procédés Solid. Stabil. Déchets. 436-.

Bourcier W.L., Knauss K.G., Merzbacher C.I. (1989). A kinetic model for the dissolution of borosilicate glass. Water-Rock Interact. 107-.

Bradley J.P., Bates J.K. (1990). Leached nuclear waste glasses: Ultramicrotomy and electron microscopic characterization. Microbeam Anal. 313-.

Buck E.C., Fortner J.A., Bates J.K., Feng X., Dietz N.L, Bradley C.R., Tani B.S. (1994). Analytical electron microscopy examination of solid reaction products in long-term tests of SRL 200 waste glasses. Mat. Res. Soc. Symp. Proc. 333, 585-.

BUWAL (1990). Eluat Test nach TVA. BUWAL, Bern, Switzerland.

BUWAL (1996). TVA/OTD: Technische Verordnung über Abfälle/Ordonnance sur le Traitement des Déchets, #814.015. BUWAL, Bern, Switzerland.

BUWAL (1998). Die Rückstände der Verbrennung; Flugasche und Filterkuchen. Umwelt-Materialien #100. BUWAL, Bern, Switzerland.

Charles R.J. (1958). Static fatigue of glass. J. Appl. Phys. 29, 1549-.

Cheron P., Chevalier P., Do Quang R., Tanguy G., Sourrouille M., Woigner S., Senoo M., Banka T., Kuramoto K., Yamaguchi T., Shimizu K., Fillet C., Jacquet-Francillon N., Godard J., Dussossoy J.-L., Pacaud F., Charbonnel J.-G. (1995). Examination and testing of an active glass sample produced by COGEMA. Mat. Res. Soc. Symp. Proc. 353, 55-.

Clark D.E., Schulz R.L., Wicks G.G., Lodding A.R. (1994). Waste glass alteration processes, surface layer evolution and rate limiting steps. Mat. Res. Soc. Symp. Proc. 333, 107-.

Clark D.E., Zoitos B.K. (1992). Corrosion of glass, ceramics and ceramic superconductors; principles, testing, characterization and applications. Noyes Publications, Park Ridge.

Colombel P. (1996). Etude du comportement à long terme de vitrifiats de REFIOM. PhD dissertation, University of Poitiers, France.

Colombel P., Godon N., Vernaz E., Thomassin J.-H. (1997). Mécanismes d'altération des vitrifiats de REFIOM et analogie avec d'autres verres industriels ou naturels. Proc. Procédés de Solidification et de Stabilisation des Déchets (Cases J.-M., Thomas F., eds.), Nancy, France, 450-.

Crovisier J-L., Honnorez J., Eberhart J.-P. (1987). Dissolution of basaltic glass in seawater: Mechanism and Rate. Geochim. Cosmochim. Acta 51, 2977-.

Crovisier J-L., Vernaz E., Dussossoy J-L., Caurel J. (1992). Early phyllosilicates formed by alteration of R7T7 glass in water at 250°C. Appl. Clay Sci. 7, 47-.

Cunnane J.C., Allison J.M. (1994). High-level waste glass compendium; what it tells us concerning the durability of borosilicate waste glass. Mat. Res. Soc. Symp. Proc. 333, 3-.

Cunnane J.C., Bates J.K., Ebert W.L., Feng X., Mazer J.J., Wronkiewicz D.J., Sproull J., Bourcier W.L., McGrail B.P. (1993). High-level nuclear-waste borosilicate glass: A compendium of characteristics. Mat. Res. Soc. Symp. Proc. 294, 225-.

Darab J.G., Feng X., Linehan J.C., Smith P.A., Roth I. (1996). Composition-structure relationships in model Hanford low-level waste glasses. Ceram. Trans. 72, 103-.

Depmeier L., Tomschi U., Vetter G. (1997). Elutionsverhalten von Reststoffen aus der thermischen Abfallbehandlung. Müll Abfall 9, 528-.

Dietzel A.H. (1988). The history of the structure of glass from the early days to present thinking. Adv. Fusion Glass 1.1-.

Dran J.-C., Petit J.-C., Trotignon L., Paccagnella A., Della Mea G. (1989). Hydration mechanisms of silicate glasses: Discussion of the respective role of ion exchange and water permeation. Mat. Res. Soc. Symp. Proc. 127, 25-.

Ebert W. L., Mazer J.J. (1994). Laboratory testing of waste glass aqueous corrosion: effects of experimental parameters. Mat. Res. Soc. Symp. Proc. 333, 27-.

EKESA (1992). Emissionsabschätzung für Kehrichtschlacke; Projekt EKESA; Schlussbericht. Auftraggebergemeinschaft für das Projekt EKESA, Switzerland.

Ewing R.C. (1996). Glass as a waste form and vitrification technology: Summary of an international workshop. National Research Council, National Academy Press, Washington.

Feng X., Cunnane J.C., Bates J.K. (1994). A literature review of surface alteration layer effects on waste glass behavior. Ceram. Trans. 39, 341-.

Fillet S. (1987). Mécanismes de corrosion et comportement des actinides dans le verre nucléaire R7T7. PhD dissertation, University Montpellier II, Montpellier, France.

Finet C. (1994). La vitrification: un procédé de banalisation des résidus de l'épuration des fumées d'incinération des ordures ménagères. TSM 4, 196-.

Flintoff J.F., Harker A.B. (1985). Detailed processes of surface layer formation in borosilicate waste glass dissolution. Mat. Res. Soc. Symp. Proc. 44, 147-.

Garland J.A., White W.B. (1985). Determination of early stages of glass dissolution by pH titration.Mat. Res. Soc. Symp. Proc. 44, 81-.

Gillies K.J.S., Cox G.A. (1988). Decay of medieval stained glass at York, Canterbury and Carlisle; II. Relationship between the composition of the glass, its durability and the weathering products. Glasstech. Ber. 61, 101-.

Gíslason S.R., Veblen D.R., Livi K.J.T. (1993). Experimental meteoric water-basalt interactions: Characterization and interpretation of alteration products. Geochim. Cosmochim. Acta 57, 1459-.

Gong W.L., Ewing R.C., Wang L.M., Vernaz E., Bates J.K., Ebert W.L. (1996). Mat. Res. Soc. Symp. Proc. 412, 197-.

Grambow B. (1985). A general rate equation for nuclear waste glass corrosion. Mat. Res. Soc. Symp. Proc. 44, 16-.

Grambow B. (1992). Geochemical approach to glass dissolution. In: Corrosion of Glass, Ceramics and Ceramic Superconductors; Principles, Testing, Characterization and Applications (Clark D.E., Zoitos B.K., eds.). Noyes, Park Ridge, U.S.A., 124-.

Grambow B. (1994). Remaining uncertainties in predicting long-term performance of nuclear waste glass from experiments. Mat. Res. Soc. Symp. Proc. 333, 167-.

Grauer R. (1985). Synthesis of recent investigations on corrosion behaviour of radioactive waste glasses. Technical Report 85-27. Nagra, Würenlingen, Switzerland.

Gutmann R. (1996). Thermal technologies to convert solid waste residuals into technical glass products. Glastech. Ber. 69, 285-.

Guyonnet D., Côme B., Ouvry J.-F., Barrès M. (1998). Concepts de stockage de déchets; un essai de définition dans une logique d'impact. Déchets Sci. Tech. 9, 39-.

Haaker R., Malow G., Offermann P. (1985). The effect of phase formation on glass leaching. Mat. Res. Soc. Symp. Proc. 44, 121-.

Jantzen C.M. (1984). Effects of Eh (oxidation potential) on borosilicate waste glass durability. Adv. Ceram. 8, 385-.

Jantzen C.M. (1988). Prediction of glass durability as a function of glass composition and test conditions: thermodynamics and kinetics. In: Proc. 1st Int. Conf. Advances Fusion Glass (D.F. Bickford *et al.*, Eds). 24.1-.

Jantzen C.M., Plodinec M.J. (1984). Thermodynamic model of natural, medieval and nuclear waste glass durability. J. Non-Cryst. Solids, 67, 207-.

Jerecinovic M.J., Kaser S., Ewing R.C. (1989). Observations of surface layers formed on basaltic and borosilicate glass: 6 month and 1 year MIIT experiments. Proc. Workshop CEC, US-DOE, CEA, 183-.

Jollivet P., Nicolas M., Vernaz E. (1998). Estimating the alteration kinetics of the French vitrified high-level waste package in a geologic repository. Nucl. Tech. 123, 67-.

Kanczarek A., Grosse-Holz G. (1996). Das Siemens-KWU-Schwel-Brenn-Verfahren. Schriftenreihe WAR 88, 77-.

Kraus F., Meunier R. (1997). Propriétés d'un vitrifiat de REFIOM produit par un procédé à arc électrique. Verre 3, 22-.

Künstler H., Klukowski C., Grotefeld V. (1994). Der VS-Kombi-Reaktor der Firma Küpat. Beih. Müll Abfall 31, 67-.

Lee C.T., Clark D.E. (1985). Electrokinetics, adsorption and colloid study of simulated nuclear waste glasses leached in aqueous solutions. Mat. Res. Soc. Symp. Proc. 44, 221-.

Linard Y. (2000). Détermination des enthalpies libres de formation des verres borosilicatés; application à l'étude de l'altération des verres de confinement de déchets radioactifs. Ph.D. dissertation, Université Paris VII, Paris.

Luo J.S., Ebert W.L., Mazer J.J., Bates J.K. (1997). Simulation of natural corrosion by vapor hydration test: Seven-year results. Mat. Res. Soc. Symp. Proc. 465, 157-.

Lutze W., Ewing R.C. (1988). Summary and evaluation of nuclear waste forms. Chapter 12. In: Radioactive waste forms for the future (Lutze W., Ewing R.C., Eds). Elsevier. 699-.

Macquet C., Thomassin J.H. (1992). Archaeological glasses as modelling of the behaviour of buried nuclear waste glasses. Appl. Clay Sci., 7, 17-.

Malow G. (1982). The mechanisms for hydrothermal leaching of nuclear waste glasses: properties and evaluation of surface layers. Mat. Res. Soc. Symp. Proc. 11, 25-.

Méhu J. (1998). Comportement à long terme et écocompatibilité des déchets ultimes stabilisés; vers une stratégie environnementale unifiée. Déchets Sci. Tech. 9, 54-.

Mottl M.J., Holland H.D. (1978). Chemical exchange during hydrothermal alteration of basalt by seawater. I. Experimental results for major and minor components of seawater. Geochim. Cosmochim. Acta 42, 1103-.

Murakami T., Banba T., Jercinovic M.J., Ewing R.C. (1989). Formation and evolution of alteration layers on borosilicate and basalt glasses: Initial stage. Mat. Res. Soc. Symp. Proc. 127, 65-.

Newton R.G. (1985). The durability of glass. Glass Technol. 26, 21-.

Newton R.G., Paul A. (1980). A new approach to predicting the durability of glasses from their chemical compositions. Glass Technol. 21, 307-.

Nogues J.-L. (1984). Les mécanismes de corrosion des verres de confinement des produits de fission. PhD dissertation, University Montpellier II, Montpellier, France.

Nogues J.-L., Vernaz E.Y., Jacquet-Francillon N. (1985). Nuclear glass corrosion mechanisms applied to the French LWR reference glass. Mat. Res. Soc. Symp. Proc. 44, 89-.

O'Connor W.K., Oden L.L., Turner P.C. (1994). Vitrification of municipal waste combustor residues: Physical and chemical properties of electric arc furnace feed and products. In: Process Mineralogy XII (Petruk W., Rule A.R., Eds). 17-.

O'Keefe J.A. (1984). Natural glass. J. Non-Cryst. Solids 67, 1-.

Patze H.U. (1996). Das Noell-Konversionsverfahren zur Umwelt-Freundlichen thermischen Verwertung von Rest- und Abfallstoffen. Schriftenreihe WAR 88, 113-.

Paul A. (1977). Chemical durability of glasses. J. Mater. Sci. 12, 2246-.

Paul A. (1982). Chemistry of Glasses. Chapman and Hall, London.

Perret D., Stille P., Shields G., Crovisier J.-L., Mäder U. (2000). Long-term stability of HT materials; Report 4. SAEFL, Section Wastes, Switzerland. The CD-ROM "Long-term stability of HT material. A compendium of the static, dynamic, thermodynamic pictures of products from the high temperature treatment of municipal solid wastes and associated residues", contains the technical report in pdf format (Acrobat Reader®) and the complete set of results in xls format (Microsoft Excel®); it is available upon request to the Swiss Agency for Environment, Forests and Landscape; Section Wastes; CH-3003 Berne, Switzerland.

Perret D. Schenk K., Chardonnens M., Stille P., Mäder U. (2002). Characteristics, behavior and durability of high temperature materials. In: Municipal Solid Waste Management: Strategies and Technologies for Sustainable Solutions (Ludwig C., Hellweg S., Stucki S., Eds). Springer Verlag, Berlin, Germany. 257-.

Perret D., Crovisier J.-L., Stille P., Shields G., Mäder U., Advocat T., Schenk K., Chardonnens M. (2003). Thermodynamic stability of waste glasses compared to leaching behaviour. Appl. Geochem., in press.

Petit J.-C., Della Mea G., Dran J.-C., Magonthier M.-C., Mando P.A., Paccagnella A. (1990). Hydrated layer formation during dissolution of complex silicate glasses and minerals. Geochim. Cosmochim. Acta 54, 1941-.

Plodinec M.J. (1984). Stability of radioactive waste glasses assessed from hydration thermodynamics. Mat. Res. Soc. Symp. Proc. 26, 755-.

Plodinec M.J., Wicks G.G. (1994). Application of hydration thermodynamics to in-situ test results. Mat. Res. Soc. Symp. Proc. 333, 145-.

Scholze H. (1991). Glass, Nature, Structure, and Properties. Springer-Verlag, New York.

Scholze H., Conradt R., Engelke H., Roggendorf H. (1982). Determination of the corrosion mechanisms of high-level waste containing glass. In: Scientific Basis for Radioactive Waste Management V (Lutze W., Ed.). North-Holland, 173-.

Schumacher W., Gugat J.-A. (1994).EloMelt- und FosMelt-Verfahren thermische Behandlungskonzepte für Reststoffe aus der Müllverbrennung. Beih. Müll Abfall 31, 152-.

Shuttleworth S., Monteith J.E. (1997). The use of laser microprobe-ICP-MS in the examination of nuclear waste glasses. Mat. Res. Soc. Symp. Proc. 465, 123-.

Sproull J.F., Marra S.L., Jantzen C.M. (1994). High-level radioactive waste glass production and product description. Mat. Res. Soc. Symp. Proc. 333, 15-.

Stahlberg R. (1996). Das Thermoselect-Verfahren. Schriftenreihe WAR 88, 131-.

Stanworth J.E. (1950). Physical Properties of Glass. Clarendon Press, Oxford, England.

Sterpenich J. (1998). Altération des vitraux médiévaux, contribution à l'étude du comportement à long terme des verres de confinement. Ph.D. dissertation, Université Henri Poincaré, Nancy.

Strachan D.M., Pederson L.R., Lokken R.O. (1985). Results from the long-term interaction and modeling of SRL-131 glass with aqueous solutions. Mat. Res. Soc. Symp. Proc. 50, 195-.

Thomassin J.-H. (1995). Apport des analogues naturels, industriels ou archéologiques à la connaissance du comportement à long terme des vitrifiats de déchets toxiques. Rapport final. University of Poitiers, France.

Thomassin J.-H. (1996). Rapport CRP OESIP 96-1. University of Poitiers, Poitiers, France.

Thomé-Kozmiensky (1994). Thermische Abfallbehandlung. EF-Verlag für Energie und Umwelttechnik. Berlin.

Vernaz E., Dussosoy J.-L. (1992). Current state knowledge of nuclear waste glass corrosion mechanisms: The case of R7T7 glass. Appl. Geochem. Suppl. Issue 1, 13-.

Whitehead N.E., Seward D., Veselsky J. (1993). Mobility of trace elements and leaching rates of rhyolitic glass shards from some New Zealand tephra deposits. Appl. Geochem. 8, 235-.

Yan J., Neretnieks I. (1995). Is the glass phase dissolution rate always a limiting factor in the leaching processes of combustion residues? Sci. Tot. Environ. 172, 95-.

Yanagisawa F., Sakai H. (1988). Leaching behaviour of a simulated nuclear waste glass in groundwater of 50-240°C. Appl. Geochem. 3, 153-.

Zachariasen W.H. (1932).The atomic arrangement in glass. J. Am. Chem. Soc. 54, 3841-.

Zellmer L.A., White W.B. (1985). Characterization of hydrated surface layers on nuclear waste glasses by infrared reflectance spectroscopy. Mat. Res. Soc. Symp. Proc. 44, 73-.

Zevenbergen C., Bradley J.P., Vander Wood T., Brown R.S., van Reeuwijk L.P., Schuiling R.D. (1994a). Microanalytical investigation of mechanisms of municipal solid waste bottom ash weathering. Microbeam Anal. 3, 125-.

Zevenbergen C., Vander Wood T., Bradley J.P., van der Broeck P.F.C.W., Orbons A.J., van Reeuwijk L.P. (1994b). Morphological and chemical properties of MSWI bottom ash with respect to the glassy constituents. Hazard. Waste and Hazard. Mat. 11, 371-.

TABLES

TABLE 1: Composition of a hypothetical HT material taking into account (i) the average composition of the 23 HT samples studied, and (ii) the lower and upper average concentrations of species in each of the three families of HT processes (in-line processes; post-processes for BA; post-processes for FA).

Component	Average proportion	Minimum proportion	Maximum proportion
SiO_2 (major)	41.4%	36.8%	48.2%
Al_2O_3 (major)	16.6%	14.5%	18.1%
CaO (major)	23.1%	17.5%	27.5%
MgO (minor)	3.2%	2.7%	3.7%
Na_2O (minor)	2.9%	2.7%	3.5%
K_2O (minor)	1.0%	0.9%	1.2%
Fe_2O_3 (minor)	7.5%	4.5%	11.5%
Cr (trace)	**2212mg/kg**	**1746mg/kg**	**2674mg/kg**
Ni (trace)	**157mg/kg**	**52mg/kg**	**222mg/kg**
Cu (trace)	**997mg/kg**	**603mg/kg**	**2310mg/kg**
Zn (trace)	**3237mg/kg**	**1262mg/kg**	**4844mg/kg**
Cd (trace)	**14mg/kg**	**0.4mg/kg**	**26mg/kg**
Pb (trace)	**250mg/kg**	**81mg/kg**	**339mg/kg**

TABLE 2: Physical characteristics of the hypothetical "glassfills" and "glassroads".

	Disposal off into "glassfill"		Re-use for "glassroad" construction	
	production: 50×10^3t/yr HT	production: 700×10^3t/yr HT	production: 50×10^3t/yr HT	production: 700×10^3t/yr HT
volume of granules (density: 2.6g/cm^3)	19×10^3m^3/yr	269×10^3m^3/yr	19×10^3m^3/yr	269×10^3m^3/yr
surface of granules (diameter: 0.1-5cm)	1.2×10^9-4.6×10^5m^2/yr	1.6×10^{10}-6.5×10^6m^2/yr	1.2×10^9-4.6×10^5m^2/yr	1.6×10^{10}-6.5×10^6m^2/yr
apparent volume of pile of HT material (apparent density of HT pile: 2g/cm^3)	25×10^3m^3/yr	350×10^3m^3/yr	25×10^3m^3/yr	350×10^3m^3/yr
upper surface of HT pile	2.5×10^3m^2/yr (depth: 10m)	35×10^3m^2/yr (depth: 10m)	50×10^3m^2/yr (depth: 0.5m)	700×10^3m^2/yr (depth: 0.5m)
volume of rain through the HT pile (average rainfall: 1500mm/yr)	2.6×10^3m^3/yr (permeability: 70%)	3.7×10^4m^3/yr (permeability: 70%)	3.8×10^3m^3/yr (permeability: 5%)	5.3×10^4m^3/yr (permeability: 5%)
flow-rate through the pile of HT material	120mL/h×m^2	120mL/h×m^2	10mL/h×m^2	10mL/h×m^2

TABLE 3: Estimated average impacts of the "glassfills" and "glassroads" on the environment, under the conditions of the corrosion scenarii discussed in the text. For each scenario, the minimum and maximum impacts (concentrations, annual loads; in parentheses) are calculated according to the lower and upper concentrations of metals in the hypothetical HT material, as given in Table 1.

	Cr	Ni	Cu	Zn	Cd	Pb
Releases for a production of 5×10^4t/yr, rcorrosion = 10^{-4}g/m^2×day, granule size = 1cm (lower boundary of scenario)						
[M^{n+}] [mg/L]	**0.25** (0.2-0.3)	**0.02** (0.006-0.03)	**0.1** (0.07-0.3)	**0.36** (0.1-0.5)	**0.002** (<0.003)	**0.03** (0.009-0.04)
Load [kg/yr]	**0.9** (0.7-1.1)	**0.07** (0.02-0.09)	**0.4** (0.3-1)	**1.4** (0.5-2)	**0.006** (0.0002-0.01)	**0.1** (0.03-0.2)
Releases for a production of 7×10^5t/yr, rcorrosion = 10^{-3}g/m^2×day, granule size = 1cm (upper boundary of scenario)						
[M^{n+}] [mg/L]	**3.6** (2.8-4.3)	**0.25** (0.08-0.4)	**1.6** (1-3.7)	**5.2** (2-8)	**0.02** (<0.04)	**0.4** (0.1-0.5)
Load [kg/yr]	**130** (103-158)	**9** (3-13)	**59** (36-136)	**191** (74-286)	**0.8** (0.02-1.5)	**15** (5-20)

TABLE 4: Estimated lifetimes of the hypothetical pile of HT material subjected to realistic conditions of corrosion. Shaded areas are the least plausible conditions of operation.

	Granule size: 0.1cm	Granule size: 1cm	Granule size: 5cm
lifetime for $r_{corrosion}$ = 10^{-3}g/m^2×day (upper boundary of scenario)	1200yr (not realistic)	**12000yr**	**60000yr**
lifetime for $r_{corrosion}$ = 10^{-4}g/m^2×day (lower boundary of scenario)	**12000yr**	**120000yr**	600000yr (not realistic)

TABLE 5: Concentrations of metals (expressed in [mg/kg]) in several natural and anthropogenic materials.

	Cr	Ni	Cu	Zn	Cd	Pb
Average HT material (see Table 1)	**2212**	**157**	**997**	**3237**	**14**	**250**
Average Municipal Solid Wastes (MSW)	60	40	2000	1400	11	700
Average Bottom Ash (BA)	500	149	7880	4088	4.1	1876
Average Fly Ash (FA)	400	133	2000	24266	623	14933
Average Filter Cake (FC)	200	213	2667	3733	88	1867
Maximum concentration allowed for disposal in inert landfill (Swiss TVA guidelines)	-	500	500	1000	10	500
Average sludge of wastewater treatment plant	84	40	388	1110	2.4	133
Residues of automobile shreding	1350	900	16000	16000	87	7000
Swiss Portland cement (maximum concentration)	125	?	?	680	5.5	255
Swiss clinker (maximum)	320	?	136	530	1.5	112
Maximum concentration allowed in Swiss clinker	150	100	100	500	1.5	100
Upper continental crust (maximum)	2980	2000	87	130	0.3	20
Mid Ocean Ridge Basalt (MORB; maximum)	300	140	80	70	0.1	1
Granites (maximum)	22	15	30	60	0.13	48
Unpolluted excavation material (Swiss U value)	50	50	40	150	1	50
Tolerable excavation material (Swiss T value)	250	250	250	500	5	250

TABLE 6: Annual masses of metals immobilised into anthropogenic materials produced in Switzerland (expressed in [t/yr]).

	Cr	Ni	Cu	Zn	Cd	Pb
Average HT material, production = 700000t/yr	**1548**	**110**	**698**	**2266**	**10**	**175**
Average HT material, production = 50000t/yr	**111**	**8**	**50**	**162**	**1**	**13**
Average Municipal Solid Wastes (MSW)	186	124	6200	4340	34.1	2200
Average Bottom Ash (BA)	386	115	6100	3200	3.4	1500
Average Fly Ash (FA)	19	6.2	93	1100	29	694
Average Filter Cake (FC)	2.3	2.5	31	43.4	1	21.7
Average sludge of wastewater treatment plant	18	8.5	82	234	0.5	28
Residues of automobile shreding	52	34	611	611	3.3	267
Swiss Portland cement (maximum concentration)	431	?	?	2344	19	879

TABLE 7: Annual losses of metals in the environment. Losses are expressed in [t/yr] (total loadings) and in [kg/yr×km^2] (surface-weighted loadings). Surface-weighted loadings take into account the maximum surfaces of soils which are concerned by the use of fertilisers in Switzerland, respectively the surface of "glassfills" or "glassroads" necessary to account for the annual production of HT material.

Total loadings [t/yr]	Cr	Ni	Cu	Zn	Cd	Pb
Average HT material, 7×10^{5}t/yr, r = 10^{-3}g/m^2×day	**0.13**	**<0.01**	**<0.06**	**0.2**	**<0.001**	**<0.02**
Average HT material, 5×10^{4}t/yr, r = 10^{-4}g/m^2×day	**<0.001**	**<0.001**	**<0.001**	**<0.002**	**<0.001**	**<0.001**
Average sludge of wastewater treatment plant	8.7	3.8	41	132	0.22	15.9
Average mineral fertilisers	130	4.7	7	45	1	4.3
Average compost	2	1.3	3.5	12	0.03	3.8
Average animal manures	-	-	80	420	0.4	8.3
Other average fertilisers made of wastes	3.7	4.1	6.5	37	0.3	6
Rhine River flux to the outlet of Switzerland	-	-	103	257	-	60
Rhône River flux to the inlet of Lake Geneva	42	93	46	264	0.9	60
Surface-weighted loadings [kg/yr×km^2]	Cr	Ni	Cu	Zn	Cd	Pb
Average HT material, "glassfill", r=10^{-3}g/m^2×day	**3726**	**265**	**1680**	**5453**	**24**	**421**
Average HT material, "glassroad", r=10^{-4}g/m^2×day	**19**	**1.3**	**8.4**	**27**	**0.12**	**2.1**
Average sludge of wastewater treatment plant	11	5	52	165	0.28	20
Average mineral fertilisers	33	1.2	1.8	11	0.25	1.1
Average compost	2	1.3	3.5	12	0.03	3.8
Average animal manures	-	-	10	53	0.05	1

FIGURE CAPTIONS

Figure 1: Schematic representation of the evolution of the entropy of materials, from the natural ressources to the production of wastes and residues, via the fabrication of domestic goods.

Figure 2: Schematic composite picture of HT materials, taking into account their static picture (physico-chemical characteristics), the dynamic picture (behaviour during corrosion), and the thermodynamic picture (computed stability). HT materials within the inner sphere are globally favourable to the environment; HT materials without the outer sphere are globally detrimental to the environment.

Figure 3: Classification of HT samples on the basis of the input material from which they are produced. In-line processes directly transform MSW into HT material. Post-processes transform residues of MSW incineration (BA, FA, FC, or mixtures of them with possible additives).

Figure 4: Examples of typical HT materials in their original state (top photographs, bottom photographs; samples on a 10 cm^2 scaling grid), and after grinding to 100-125μm (micrographs in the middle).

Figure 5: Typical X-ray diffractograms of 100-125μm ground HT materials, showing vitreous character (P8), contrasted vitreous/vitrocrystalline character (P12.2*), or vitrocrystalline character (P6*).

Figure 6: Proportions of the major and minor constituents in HT materials. Left: SiO_2 (network-forming), Al_2O_3 (network-forming or modifying) and CaO (network- modifying). Right: MgO, Na_2O, K_2O and Fe_2O_3.

Figure 7: Concentrations of several toxic and environmentally relevant metals in HT materials.

Figure 8: Summary of the physical, chemical and microscopic features of HT materials. Samples at the union of the three circles (P7, P9.1, P12.1, P14) have the best static characteristics. Samples at the outside of the circles have less favourable characteristics.

Figure 9: Schematic of the mechanisms of corrosion taking place when a glass is subjected to water.

Figure 10: Scanning electron micrographs of the surface features of 100-125 μm ground HT materials prior to (small micrographs) and after 10 days corrosion (large micrographs). Corroded sample P7 exhibits pits but almost no secondary mineral phases; corroded sample P16* shows a dense distribution of secondary minerals above the gel layer.

Figure 11: (a) Concentration of Si in the leachates of the Strasbourg test after 1 day corrosion at 90 °C, as a function of the pH of the leachate. (b) Relationships between the measured pH of the leachate and the proportion of CaO in HT materials, respectively the released concentration of Ca^{2+} in the leachate, after 1 day corrosion.

Figure 12: Temporal evolution of the concentrations of major (Si, Ca), minor (Na, K) and trace species (Sn, Pb) in the leachates of several HT materials corroded during 1 day, 3 days, and 10 days. The temporal fingerprint is different from sample to sample and from element to element.

Figure 13: Evolution of the apparent normalised release rates of major, minor and trace species as a function of the duration of corrosion. Although the initial rates (*i.e.* after 1 day) are different from sample to sample and from element to element, the rates measured after 10 days tend to a limiting value, whatever the HT material.

Figure 14: Comparison of the static and dynamic features of HT materials. Although most HT materials have negative characteristics with respect to their content in toxic metals, they all exhibit a highly favourable behaviour with respect to their propensity to release these metals. The three sample (P6*, P7, P11*) at the union of the circles have the highest qualities.

Figure 15: Schematic curves (top, bottom) of the calculated free energy of hydration ΔG_{hydr} of two hypothetical HT materials (Si-rich/Ca-poor, respectively Si-poor/Ca-rich) in function of the pH. The shaded areas are the actual ranges of computed ΔG_{hydr} of HT materials, categorised as a function of the HT process from which they originate. For comparison, the computed curve for the standard HLW glass SON68 is also present (dotted curve).

Figure 16: Relationship between the normalised apparent dissolution rate of HT materials and their free energy of hydration, calculated for the pH values measured after 1 day and 10 days corrosion. For comparison, the literature-extracted results (Plodinec and Wicks, 1994) obtained for 115 glasses of different origins corroded under the conditions of the MCC-1 test are reproduced.

Figure 17: Tentative semi-quantitative ranking of HT materials. For partly characterised samples, the rank may be underestimated.

Figure 18: Modelised concentrations (top) and absolute releases (bottom) of metals in the leachate of the corrosion experiments, as a function of the metal content in the HT materials and the size of the granules subjected to corrosion. Two realistic rates of corrosion are used for the computation.

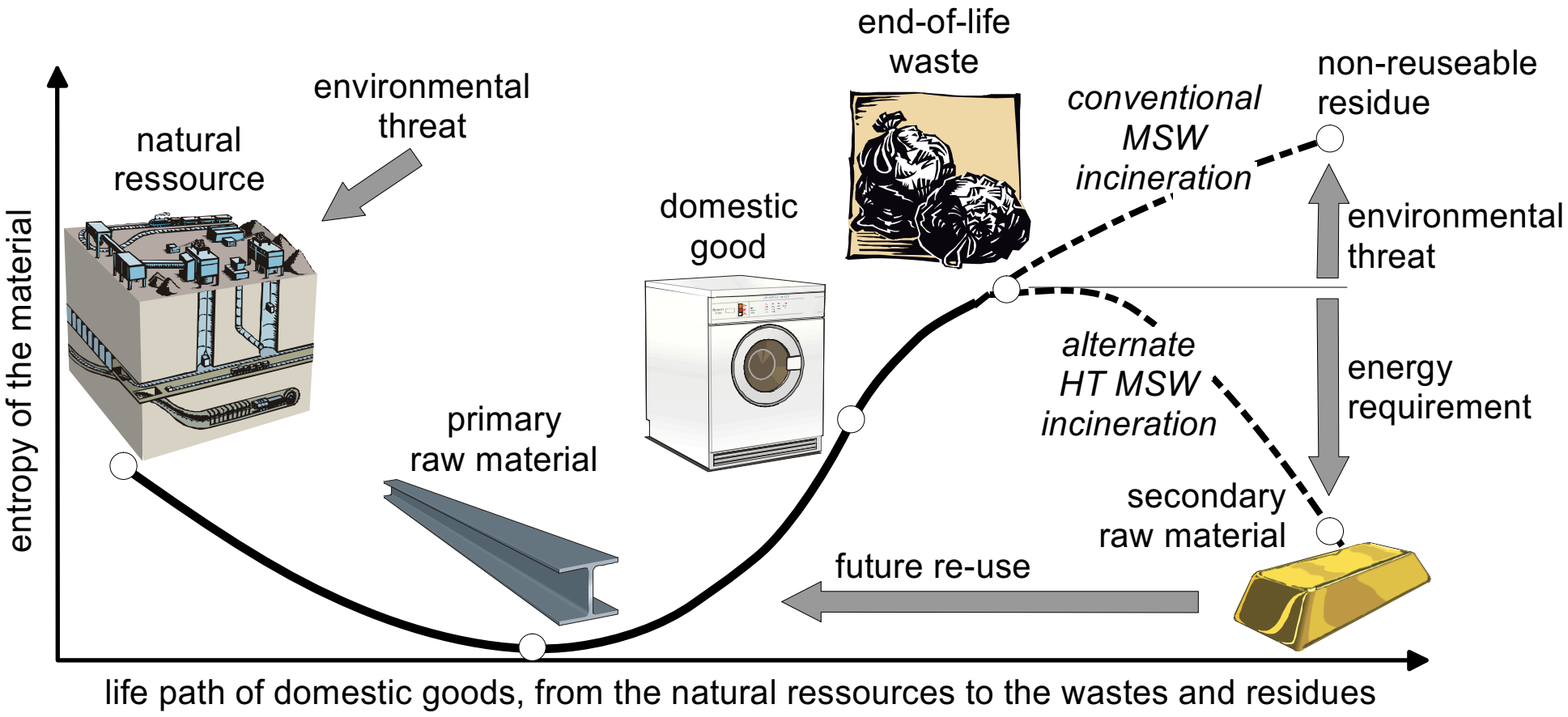

Figure 1 Perret et al.

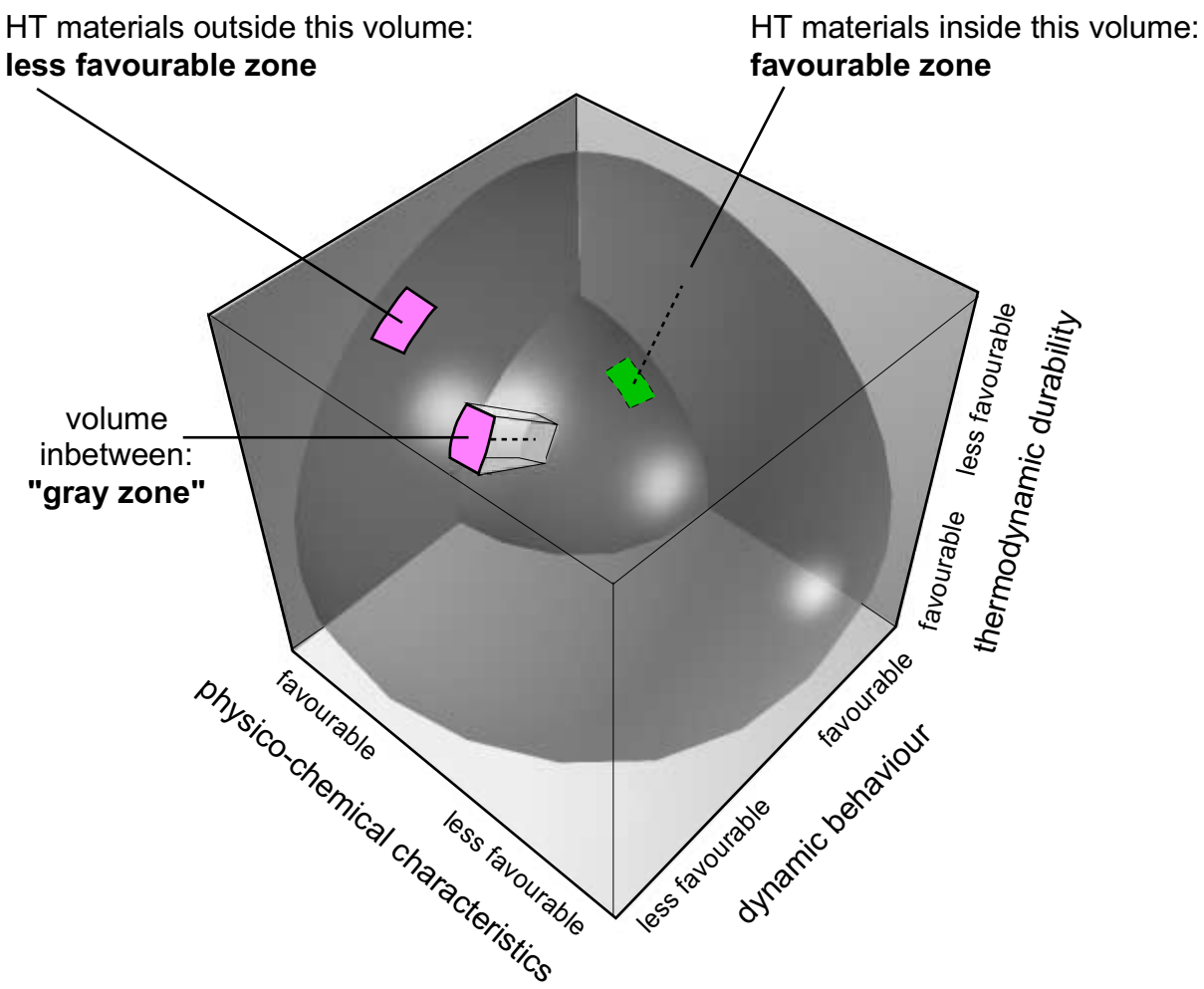

Figure 2 Perret et al.

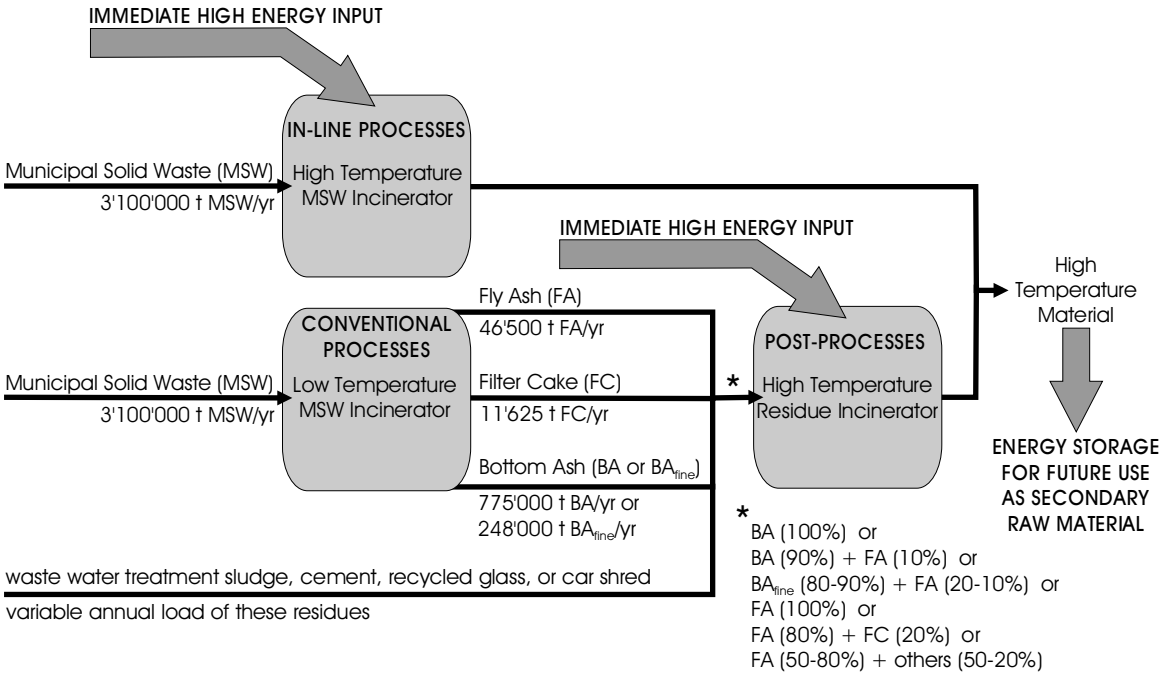

Figure 3 Perret et al.

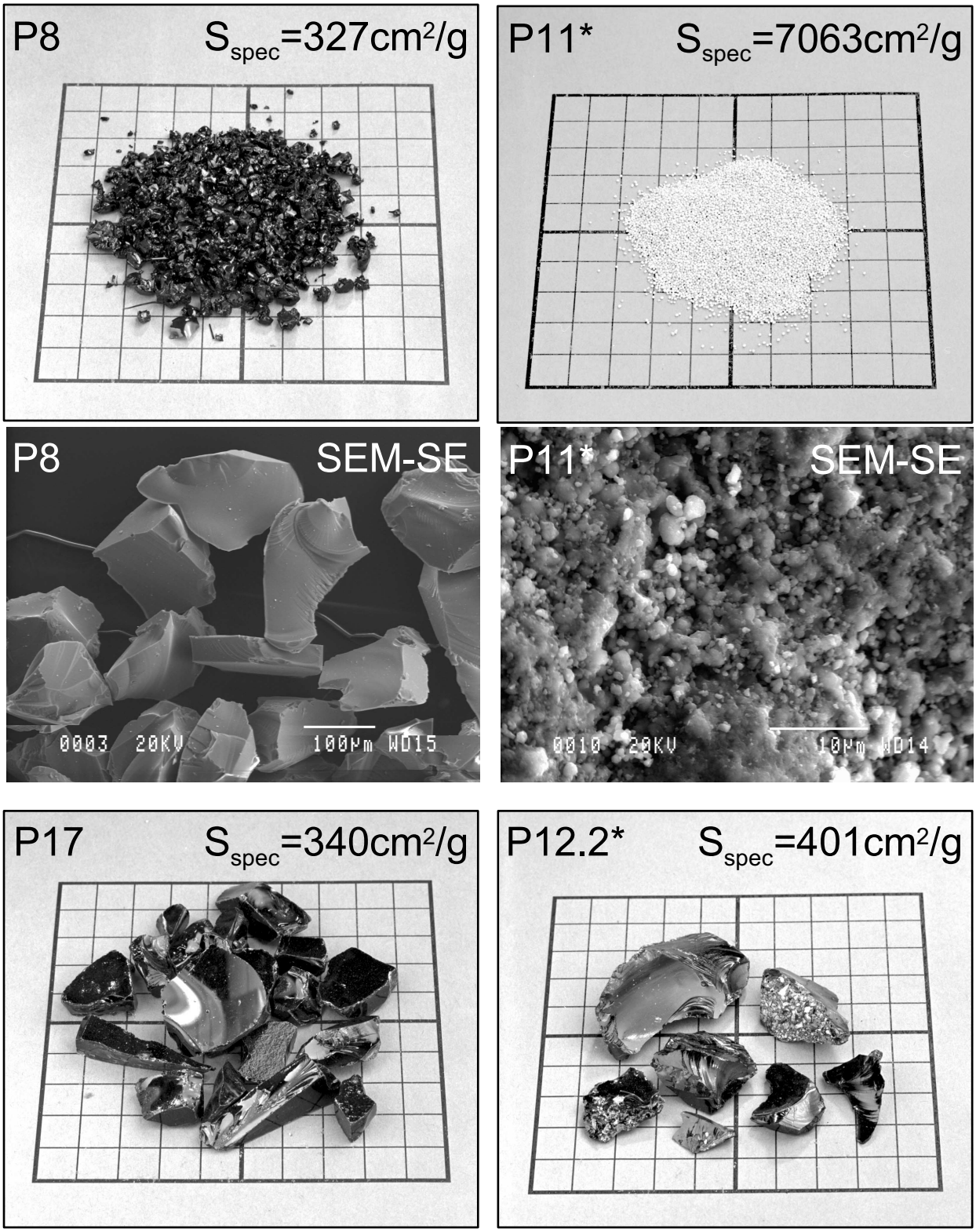

Figure 4 Perret et al.

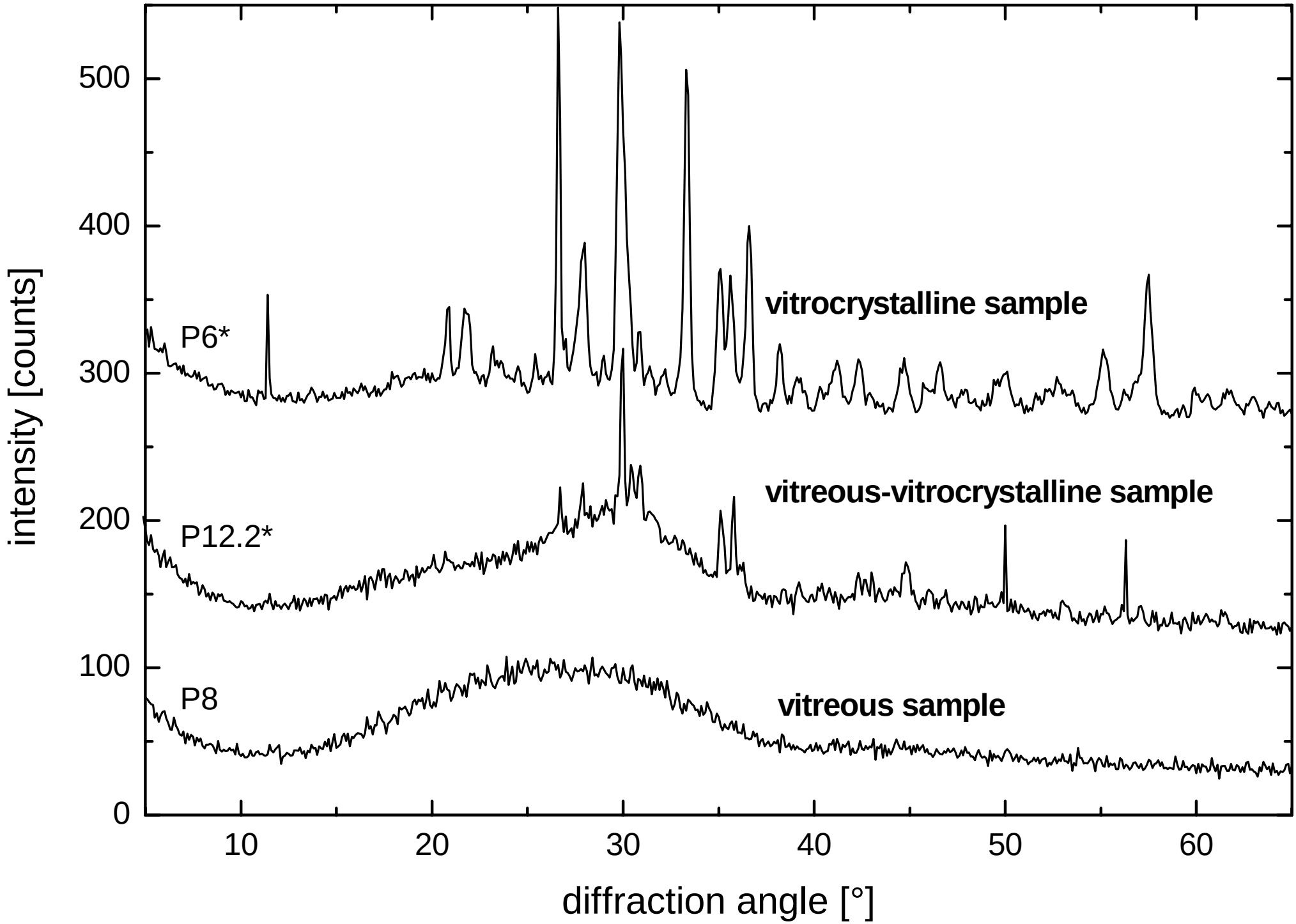

Figure 5 Perret et al.

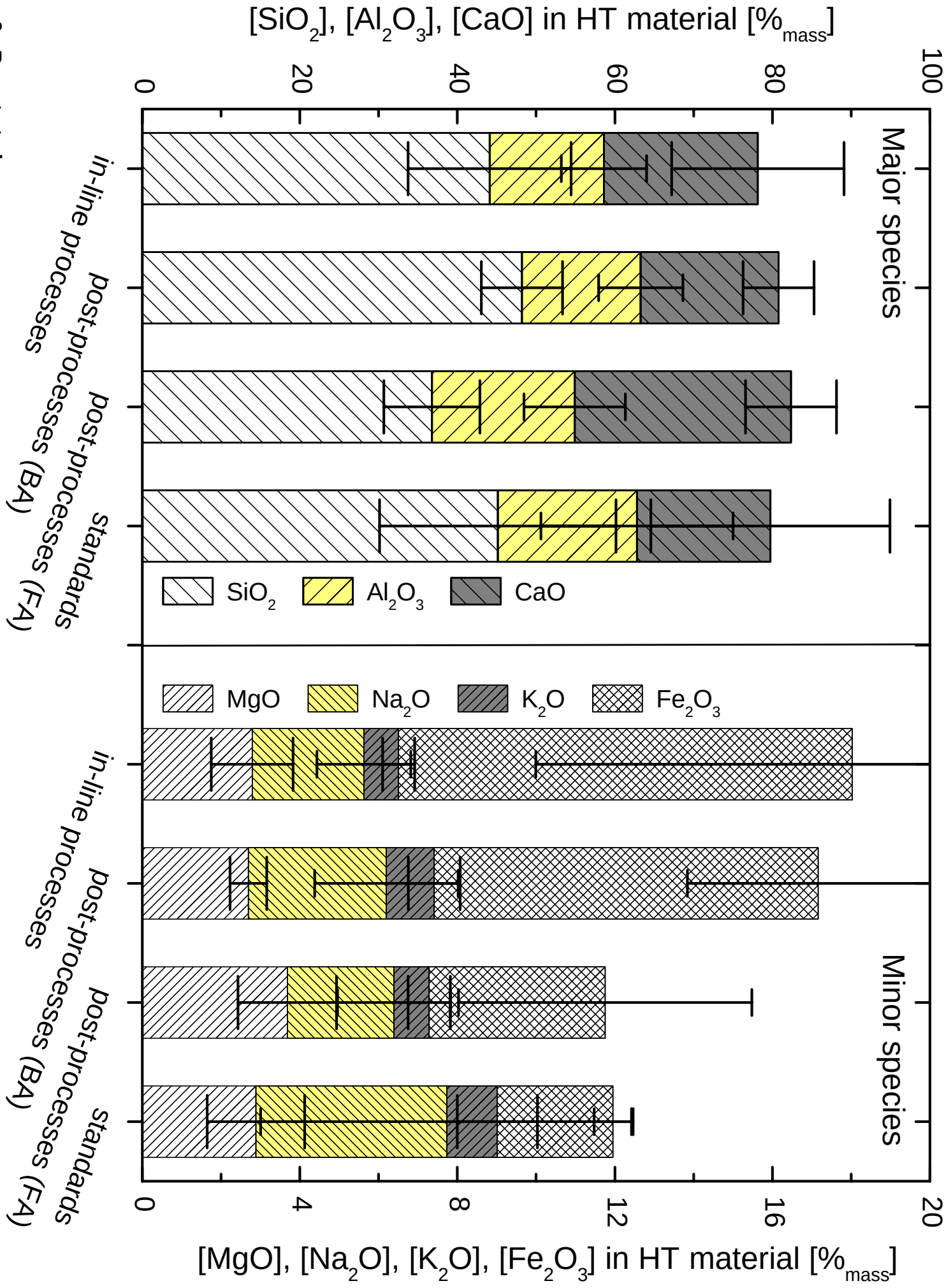

Figure 6 Perret et al.

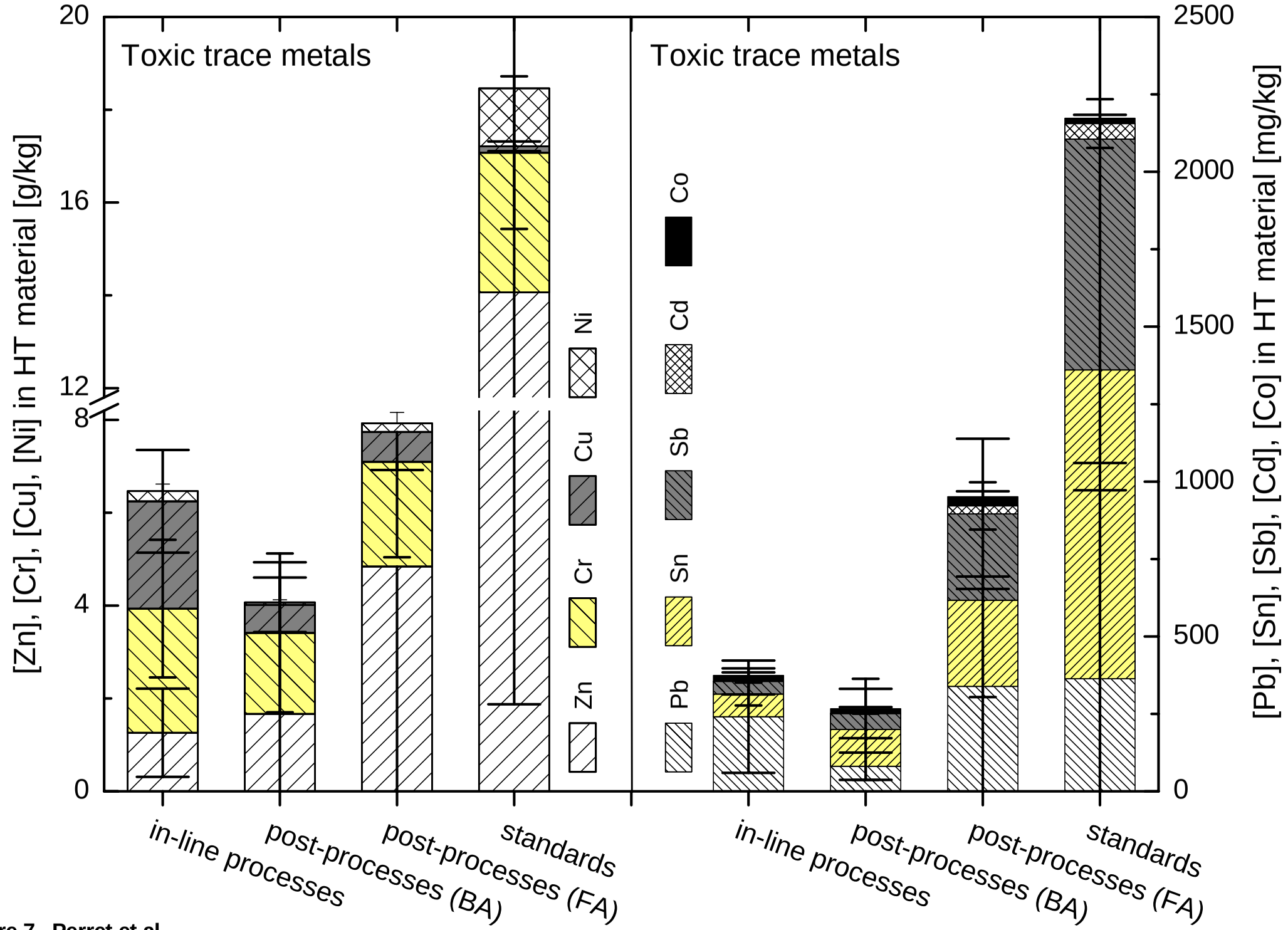

Figure 7 Perret et al.

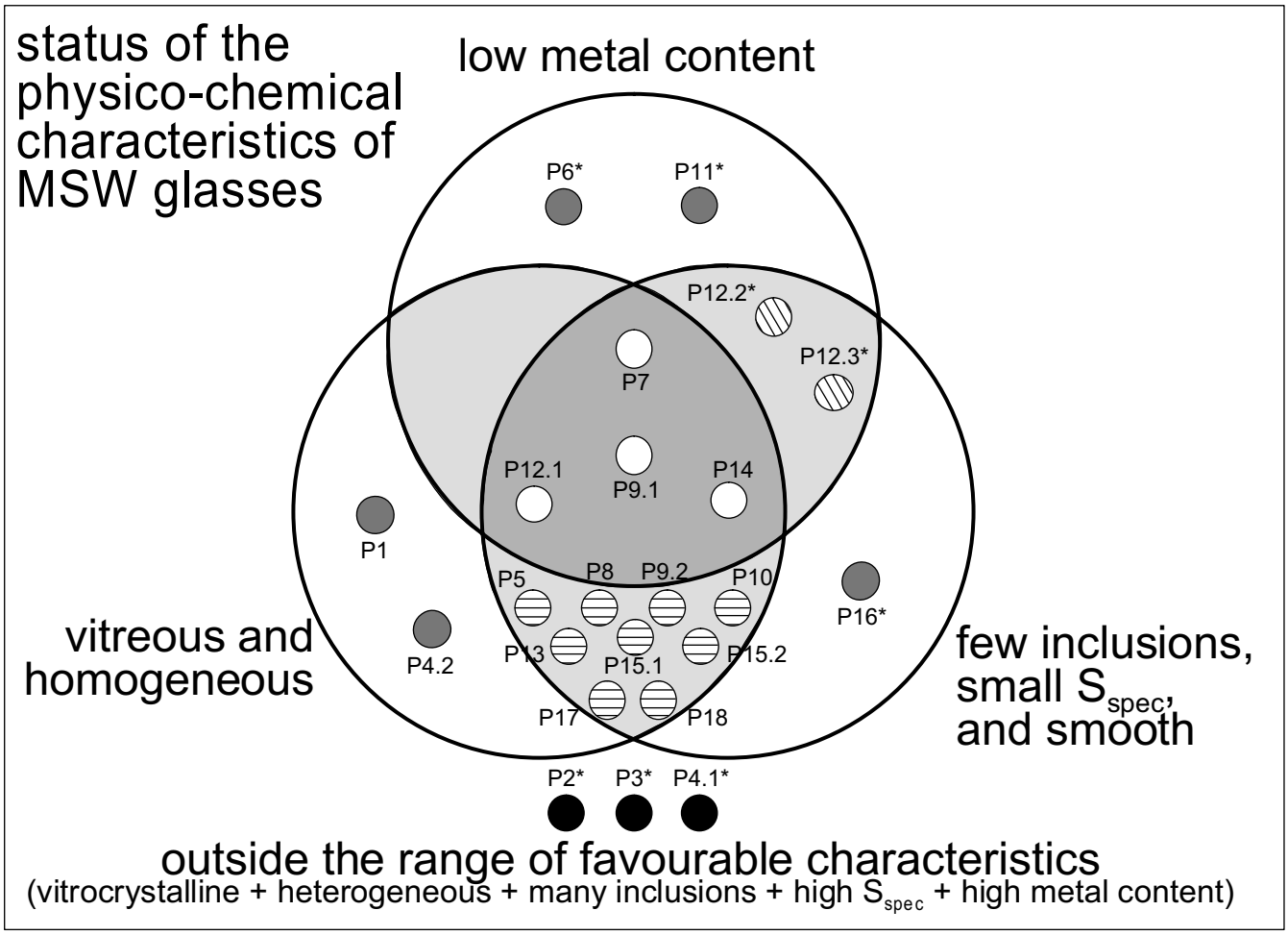

Figure 8 Perret et al.

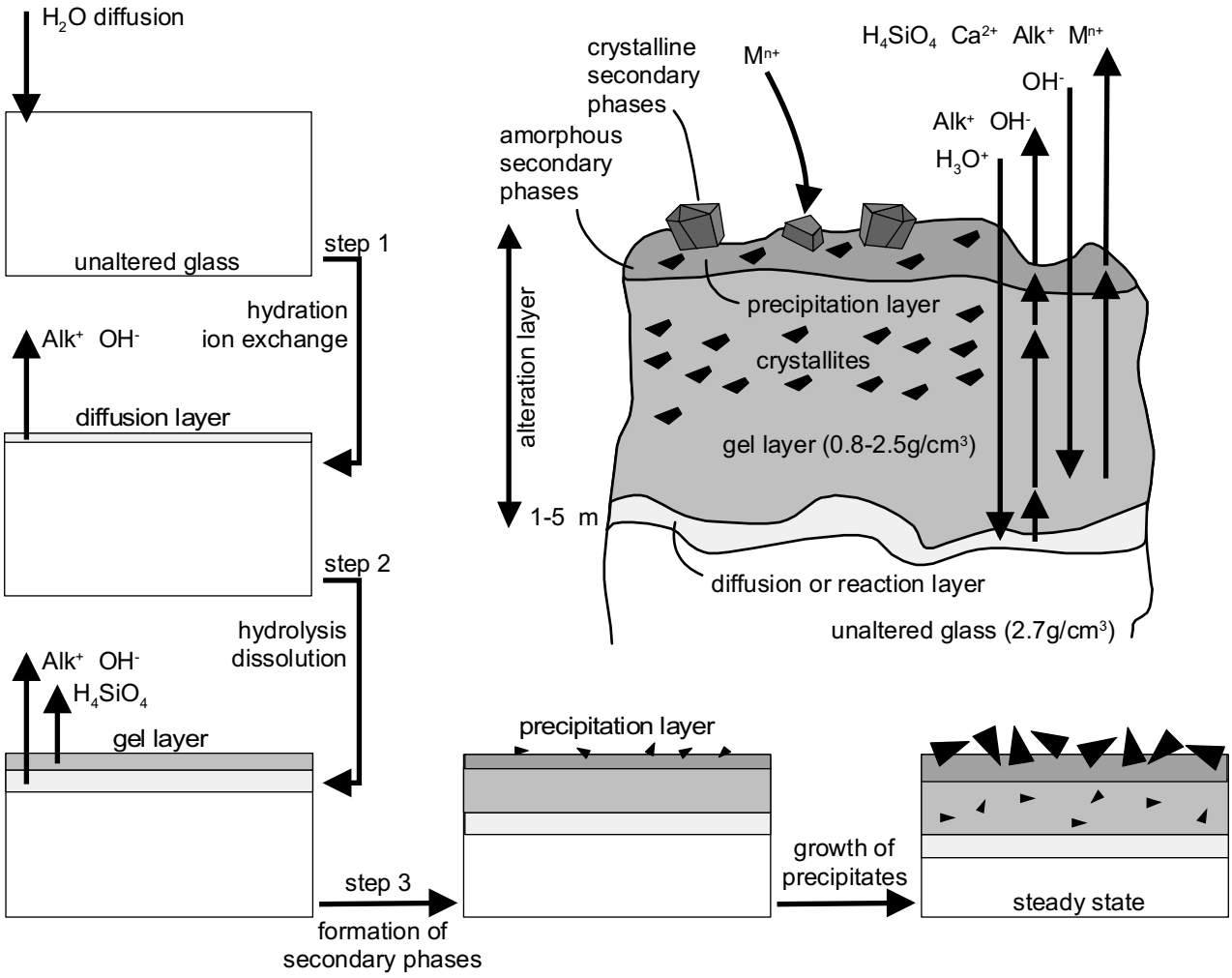

Figure 9 Perret et al.

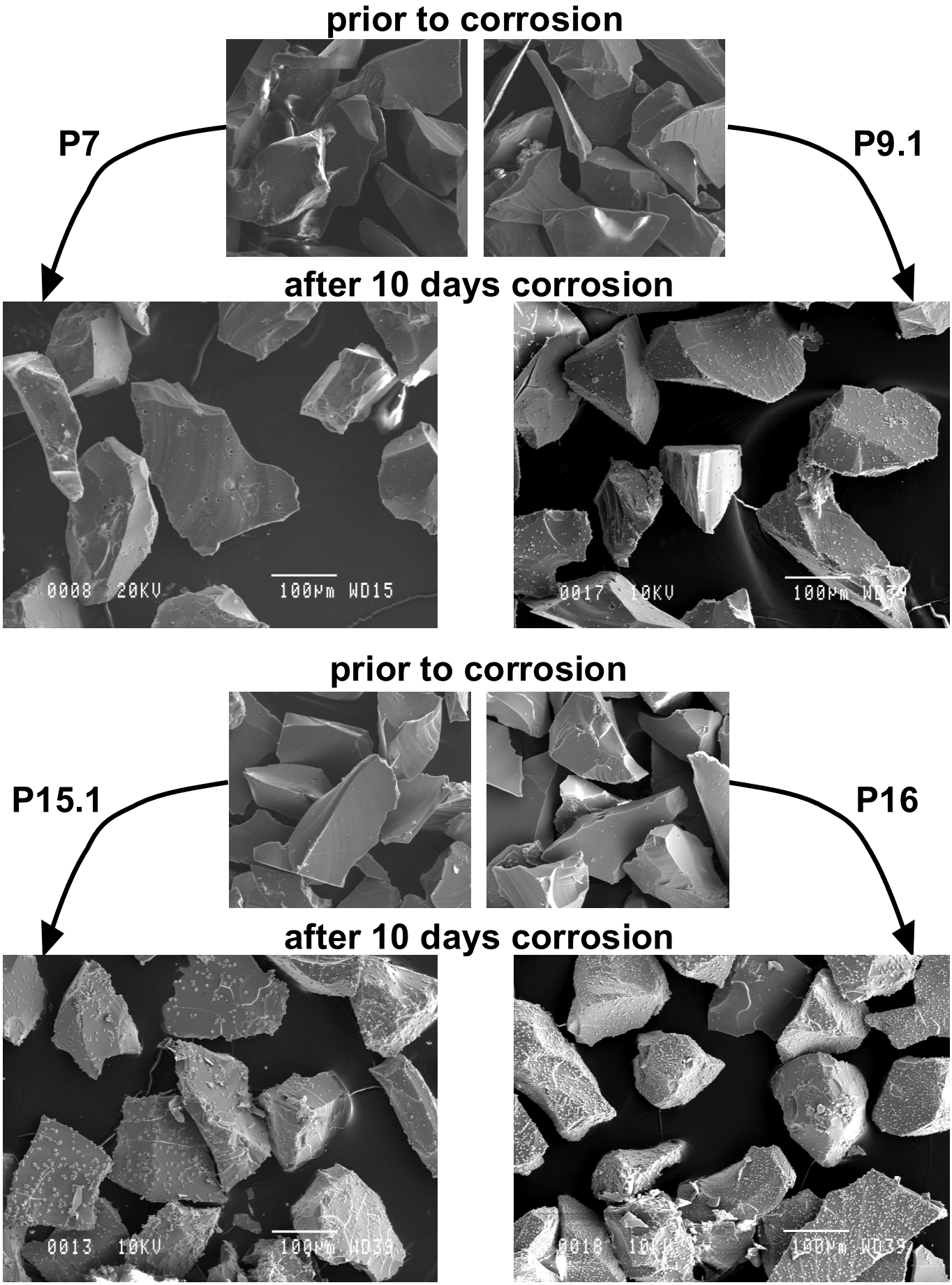

Figure 10 Perret et al.

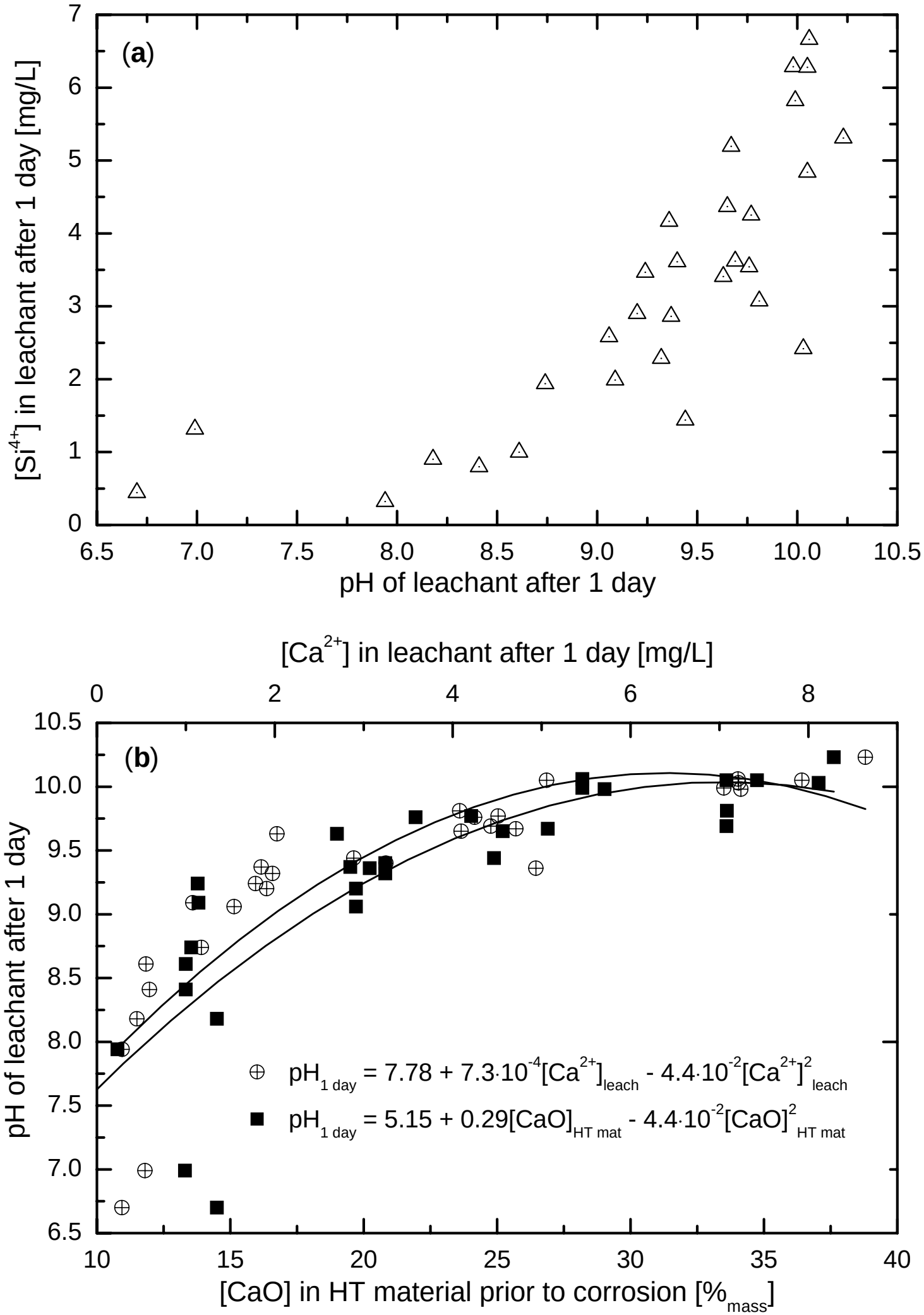

Figure 11 Perret et al.

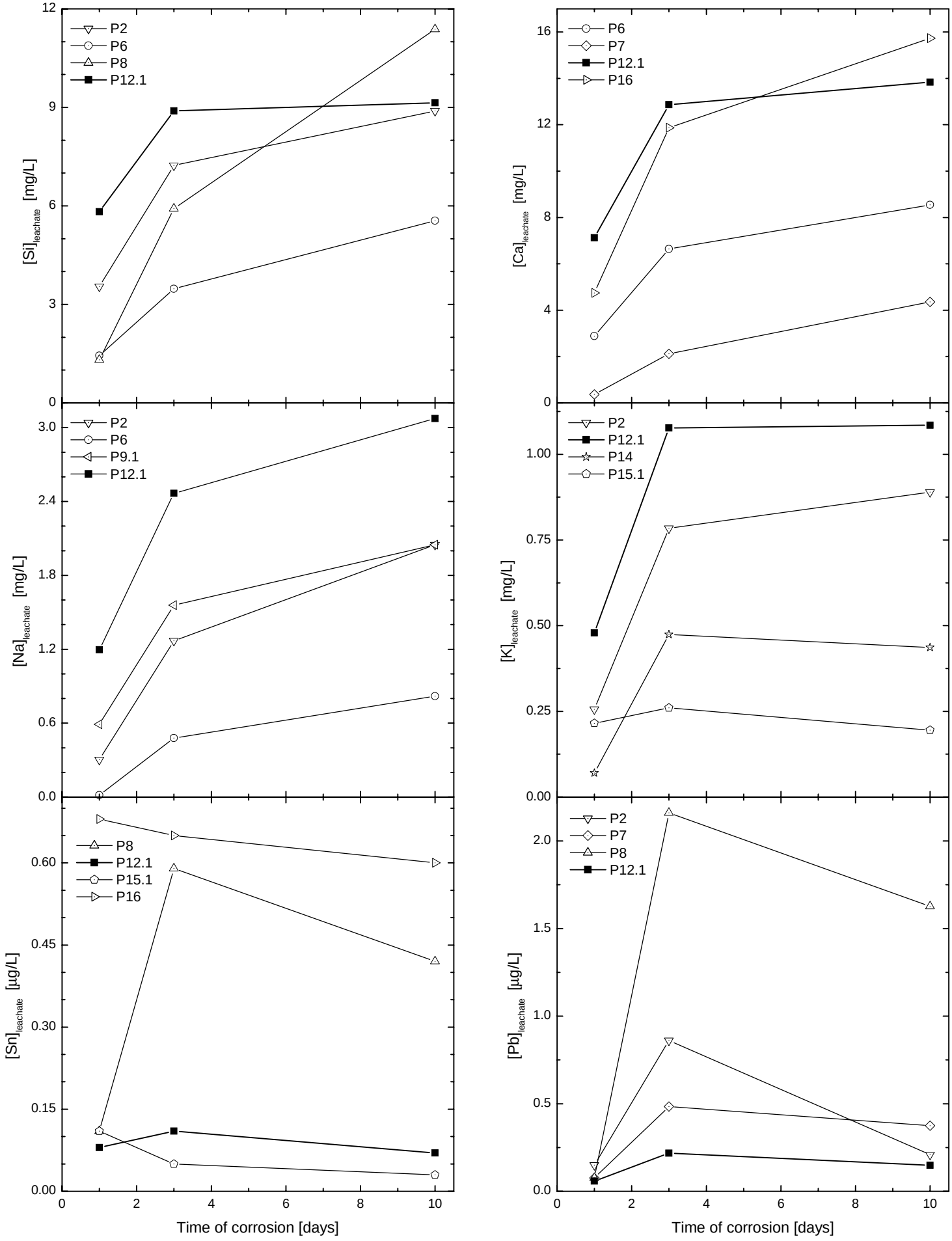

Figure 12 Perret et al.

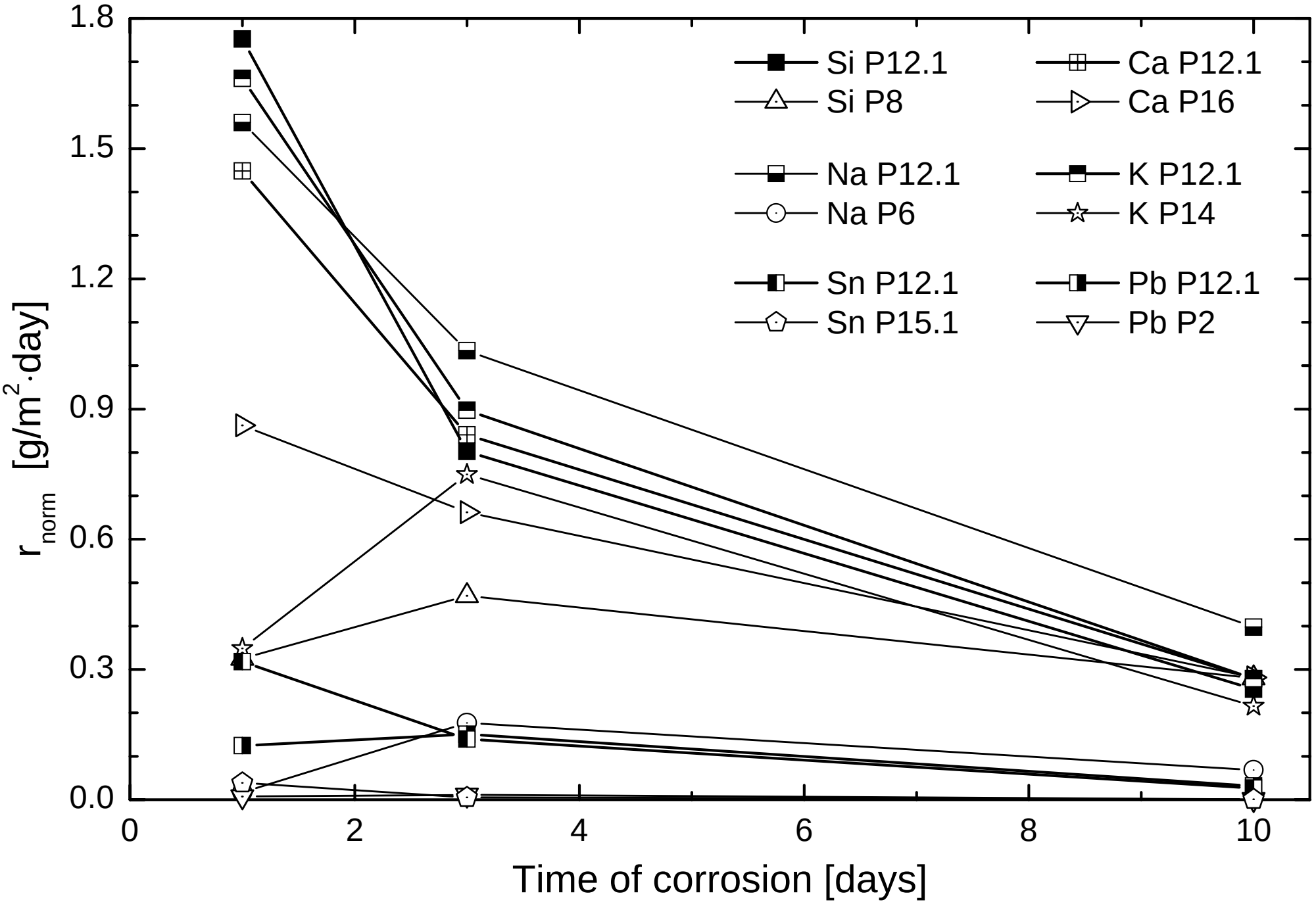

Figure 13 Perret et al.

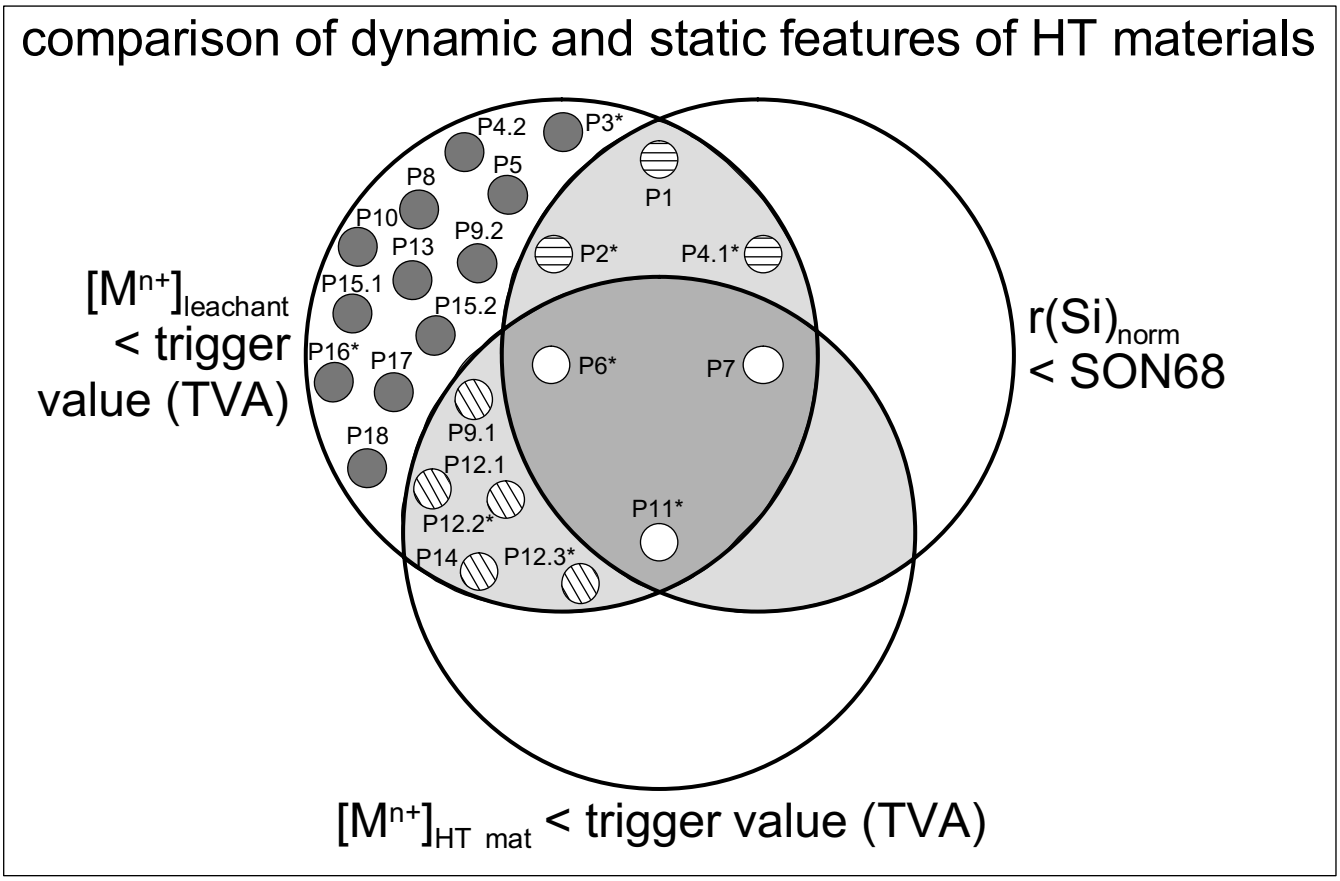

Figure 14 Perret et al.

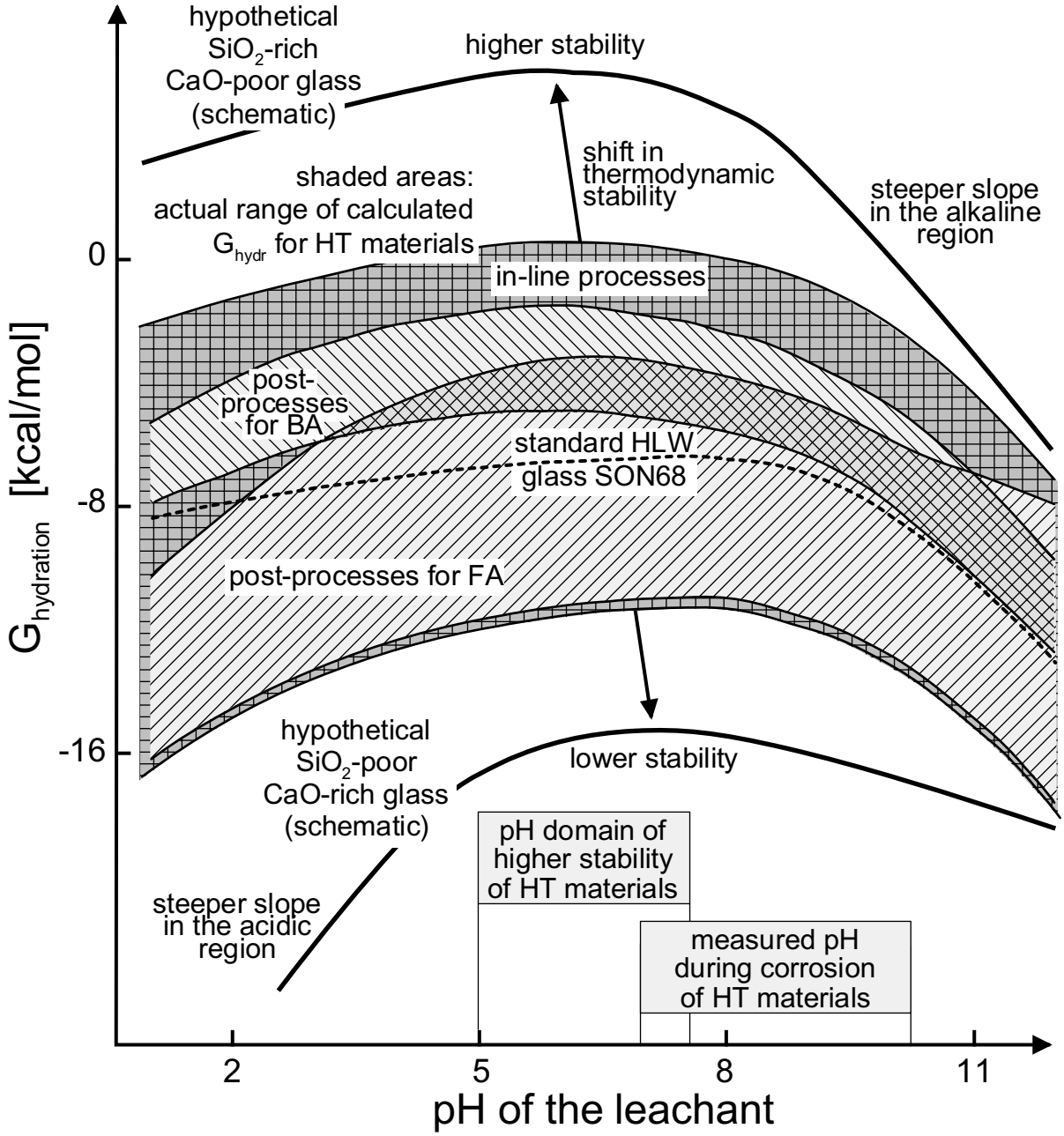

Figure 15 Perret et al.

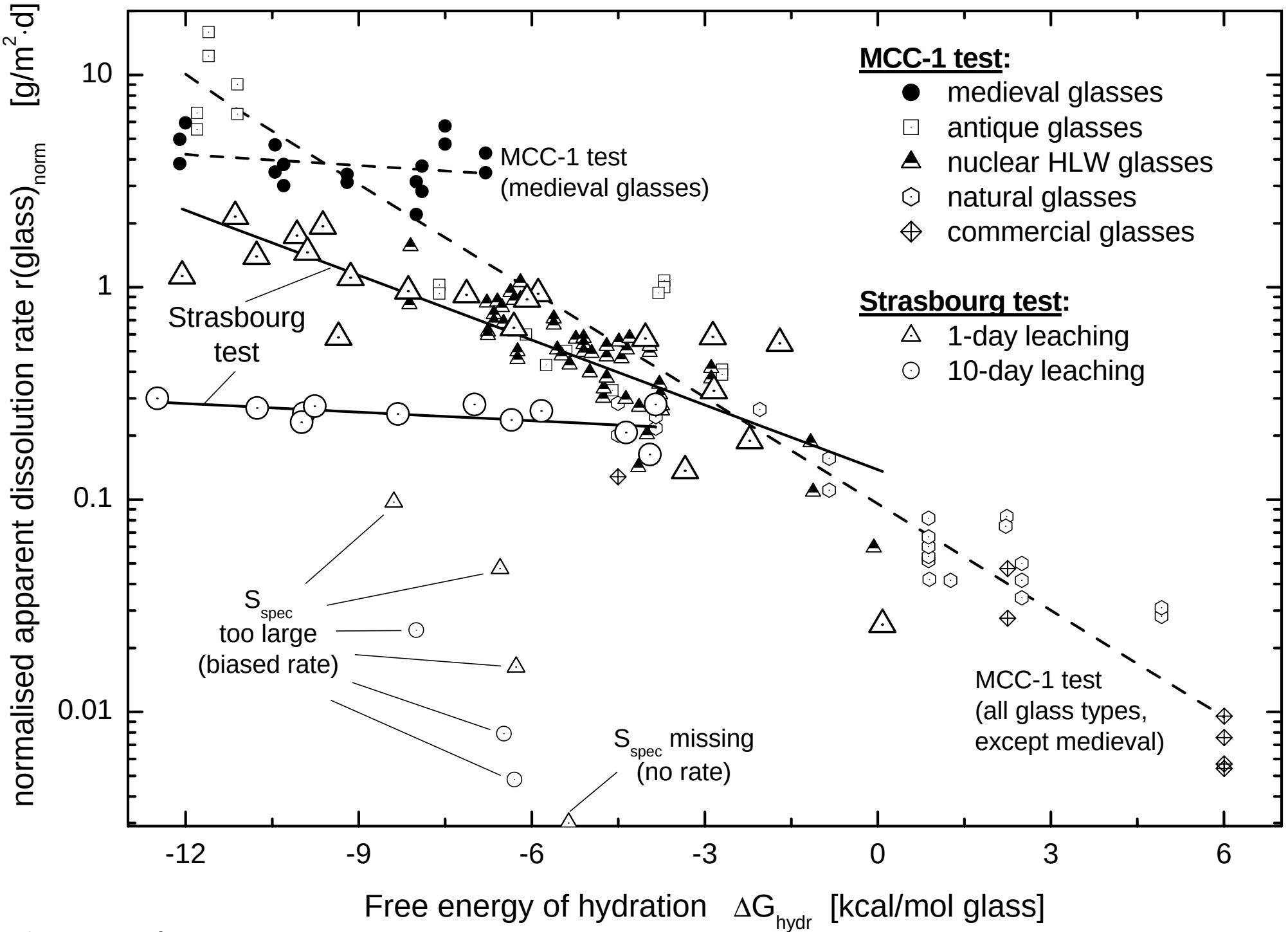

Figure 16 Perret et al.

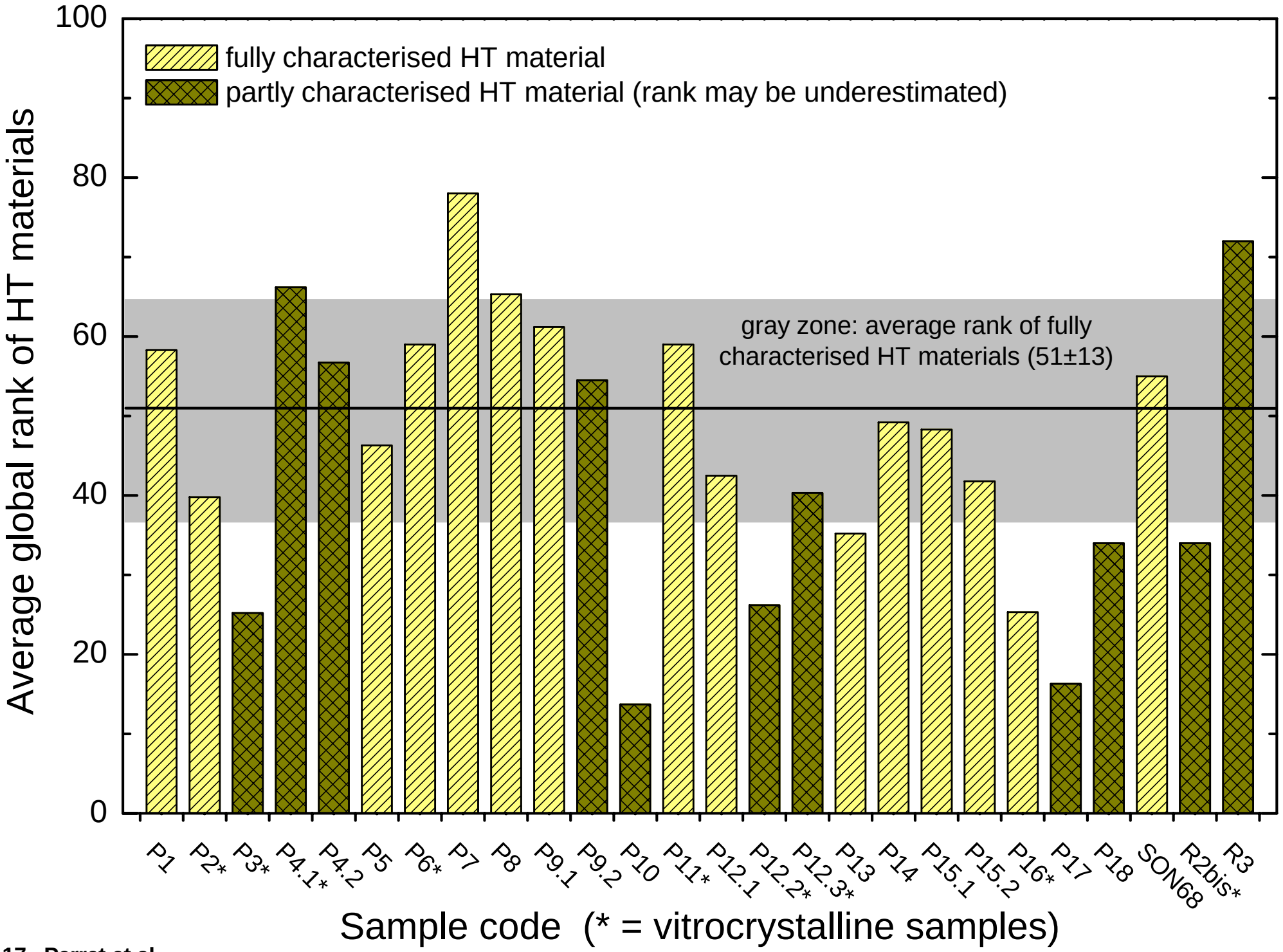

Figure 17 Perret et al.

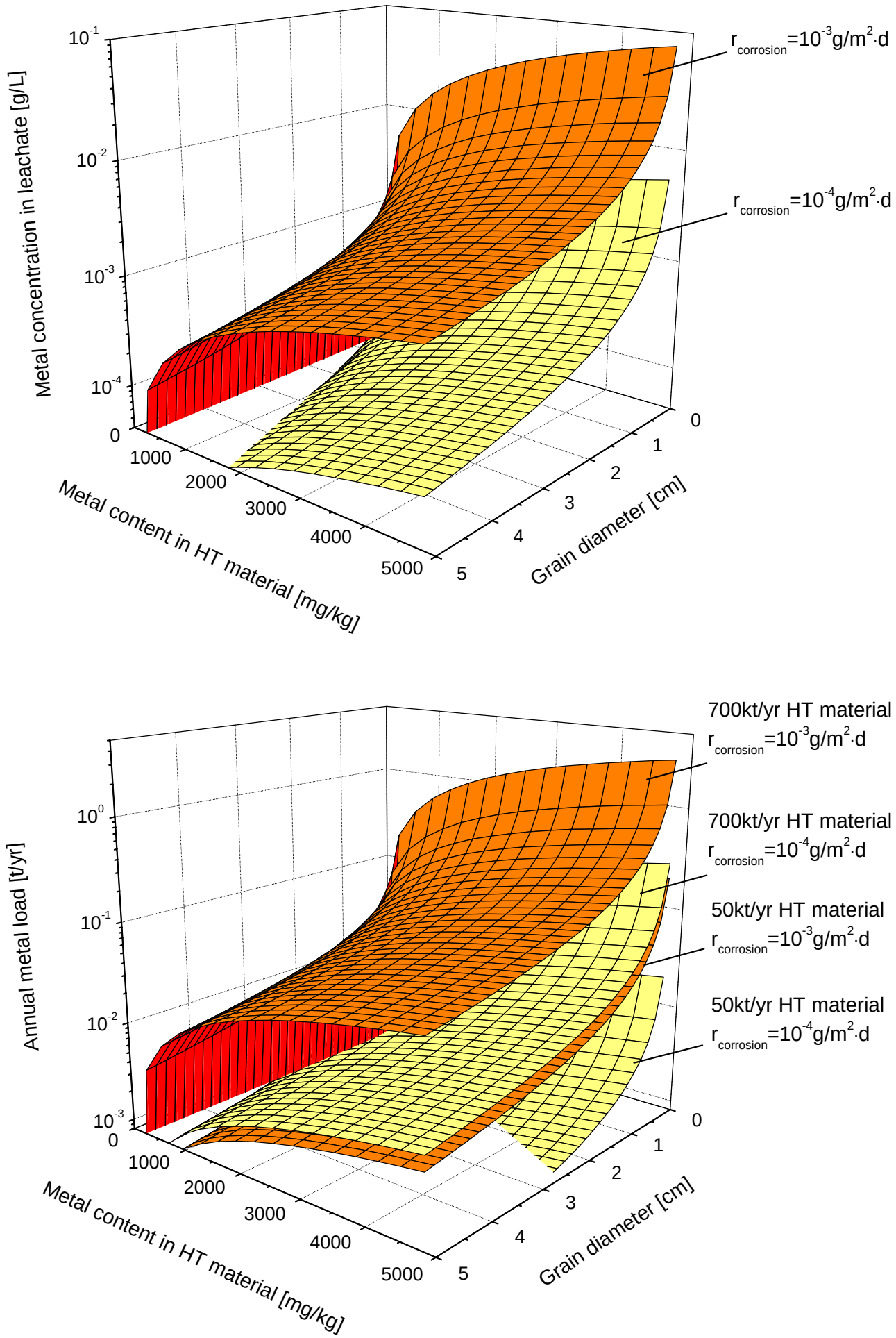

Figure 18 Perret et al.